

UC Riverside

UC Riverside Previously Published Works

Title

Soil salinization in very high-density olive orchards grown in southern Portugal: Current risks and possible trends

Permalink

<https://escholarship.org/uc/item/3np7k5vz>

Authors

Ramos, Tiago B
Darouich, Hanaa
Šimůnek, Jiří
[et al.](#)

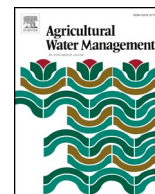
Publication Date

2019-05-01

DOI

10.1016/j.agwat.2019.02.047

Peer reviewed



Soil salinization in very high-density olive orchards grown in southern Portugal: Current risks and possible trends



Tiago B. Ramos^{a,*}, Hanaa Darouich^b, Jiří Šimůnek^c, Maria C. Gonçalves^d, José C. Martins^d

^a Centro de Ciência e Tecnologia do Ambiente e do Mar (MARETEC), Instituto Superior Técnico, Universidade de Lisboa, Av. Rovisco Pais, 1, 1049-001 Lisboa, Portugal

^b Centro de Investigação em Agronomia, Alimentos, Ambiente e Paisagem (LEAF), Instituto Superior de Agronomia, Universidade de Lisboa, Tapada da Ajuda, 1349-017 Lisboa, Portugal

^c University of California Riverside, Riverside, CA 92521, USA

^d Instituto Nacional de Investigação Agrária e Veterinária (INIAV), Av. República, 2780-157 Oeiras, Portugal

ARTICLE INFO

Keywords:

Alentejo region
Electrical conductivity
HYDRUS-1D
Multicomponent solute transport
Sodium adsorption ratio

ABSTRACT

Deficit irrigation practices carried out in very high-density olive orchards grown in the Alentejo region of southern Portugal can bring important economic benefits in terms of water savings, yields, and oils. They can also result in serious salinization/sodification problems without proper management of soil and water resources. The main objective of this study was to evaluate the long-term (30 years) impact of those irrigation practices on local soil resources using a multicomponent transport modeling approach embedded in the HYDRUS-1D model. Soil salinization and sodification risks were quantified for 160 soil profiles by considering eight different scenarios: current monitored irrigation practices (S1), using waters of variable quality (S2-S6), planting maize as an alternative crop (S7), and using climate change projections for the region (S8). Despite the large observed variability, simulations that considered current irrigation practices (S1) produced average values of the electrical conductivity of the soil solution (EC_{sw}) at the end of the leaching seasons always below the threshold limit for crops moderately tolerant to soil salinity. In this scenario, the average values of the sodium adsorption ratio (SAR) were also kept within the same magnitude of those determined at the beginning of the simulation period (initial conditions). Irrigations with worse quality waters (S2-S6) led to higher EC_{sw} and SAR values. Although annual rainfall amounts influenced the salinity build-up, the SAR evolution depended mainly on water quality. In maize soil profiles (S7), the simulated EC_{sw} and SAR values were lower than in olive soil profiles, with irrigation practices contributing to salt removal during the seasons. Conversely, the climate change scenario (S8) resulted in slightly higher EC_{sw} and SAR values than those simulated for current conditions, indicating a potentially greater risk of soil degradation in the near future. Although current irrigation practices seem to present relatively low soil salinization/sodification risks, the variability of results and the uncertainty associated with model predictions indicate that close monitoring to prevent further degradation of soil and water resources in the region should be recommended.

1. Introduction

Olive (*Olea europaea* L.) is a strategic crop in the Mediterranean basin, with a harvested area close to 10.3 million ha in 2016, which yielded more than 18.3 million ton of fresh fruit (FAOSTAT, 2018). Spain, Greece, Italy, Turkey, and Morocco produced over 77% of the overall production, followed by Syria, Tunisia, Algeria, Egypt, and Portugal. In these countries, olive has provided safe economic returns to farmers over the centuries, with trees being sparsely planted (< 100 trees ha^{-1}), without irrigation, but attaining acceptable yields even in poor soils due to their resistance to drought, lime, and salinity.

However, production methods have been changing rapidly since the early 1990s, with high (≥ 200 trees ha^{-1}) and very high-density (≥ 1000 trees ha^{-1}) olive orchards being now preferred to traditional systems (Santos et al., 2007; Gucci et al., 2012; Gómez-del-Campo, 2013; Lorite et al., 2018). Irrigation became a critical practice due to the higher evapotranspiration demand of the dense canopies and the low soil volume available for each tree (Villalobos et al., 2000; Ramos and Santos, 2009; Conceição et al., 2017). However, this practice has also limited the expansion of these production methods as suitable areas are mostly located in regions where water is scarce, and competition with other uses is great and increasing (Gómez-del-Campo, 2013).

* Corresponding author at: MARETEC, Instituto Superior Técnico, Av. Rovisco Pais, 1, 1049-001 Lisboa, Portugal.

E-mail addresses: tiago_ramos@netcabo.pt, tiagobramos@tecnico.ulisboa.pt (T.B. Ramos).

<https://doi.org/10.1016/j.agwat.2019.02.047>

Received 12 October 2018; Received in revised form 14 February 2019; Accepted 28 February 2019

0378-3774/© 2019 Elsevier B.V. All rights reserved.

This has so far not been the case of the Alentejo region of southern Portugal, where high and very high-density orchards have been rapidly expanding over the last few years, covering now more than 55,000 ha (DGADR, 2018) as new irrigation land becomes available with the Alqueva Project (EDIA, 2018).

The Alqueva Project initiated the conversion of new irrigation land in 2002, progressively adding 110,000 ha to the existing irrigated area in the region. At that time, state agencies projections included 42 crops to be grown in the region based on their potential added value to the country's economy (GPAA, 2004). Olive was only considered for table consumption; not for oil extraction. However, the reality followed a different direction when many agricultural companies started moving into the region to seize the opportunity given by the European Commission decision 2000/406/CE to expand the Portuguese olive tree planting quota for new orchards. This fast expansion of olive orchards has even raised plans to further expand the irrigated land by more than 50,000 ha (EDIA, 2018) due to the lower water requirements of olive orchards compared to other earlier projected crops.

Irrigation in high and very high-density orchards is fundamental to fulfill crop water requirements. However, irrigation practices also need to consider associated negative impacts of oversupply on olive productivity, oil quality, and the excessive crop set that may strongly affect vegetative growth and fruit production during the following season. Thus, the system requires accurate management in terms of light interception and the use of soil nutrients and water resources. Several studies concluded that deficit irrigation management practices, sustained or regulated, can have a positive effect on yield returns and can provide economic benefits with no significant impact on the chemical characteristics and the commercial value of olive oils (Tognetti et al., 2005; Ramos and Santos, 2010; Rosecrance et al., 2015; Ahumada-Orellana et al., 2018; Hernández et al., 2018). However, this can trigger a serious environmental problem as deficit irrigation practices, while resulting in important water savings, can also potentially promote soil salinization and sodification problems in a region where rainfall may not always be sufficient to remove the salts accumulated in the soil profile during irrigation. It is therefore important to closely monitor soil and water quality in the region, to promote efficient leaching management to counteract soil salinization, and to develop necessary tools for predicting the impact of management practices on soil and water resources in the short and long term.

A representative example of that problem is given by Peragón et al. (2018) for the province of Jaen (south of Spain), which holds a quarter of Spain's orchard surface. In this region, an irrigation volume of only 150 mm y^{-1} is assigned by water authorities for each field, which means that deficit irrigation practices are practically mandatory. While soil salinization risks are high due to the low quality of irrigation waters used in the region, promoting soil leaching may lead to a reduction in the available water for olives, thus negatively affecting yield in the short-term. In other regions of the Mediterranean basin, where water is even more scarce, and freshwater resources are primarily used for urban use, marginal waters (saline waters or wastewaters) are the only resource available for olive tree irrigation. Hence, the impact of these low-quality waters on olive yields needs to be further minimized by improving the decision-making process, namely by making available appropriate tools capable of adjusting irrigation volumes and frequencies to remove salts from the root zone (Murillo et al., 2000; Melgar et al., 2009; Aragiús et al., 2010; Ahmed et al., 2012; Ghrab et al., 2013; Tekaya et al., 2016).

Currently available modeling tools offer different solutions for managing low-quality waters and for quantifying their impact on crop yields and soil and water resources. Water balance models (Pereira et al., 2007; Domínguez et al., 2011; Rosa et al., 2016) are normally limited to the assessment of evapotranspiration and yield reductions due to the salinity stress. These models can only consider steady-state solutions that represent general impacts over extended time periods, with the detailed description of the soil salinization process, including

the salinity build-up in the soil profile being far beyond their capabilities. On the other hand, transient models (Šimůnek and Suarez, 1994; Pang and Letey, 1998; Ragab et al., 2005; van Dam et al., 2008; Šimůnek et al., 2016) have far greater capabilities, allowing for the consideration of site-specific soil, water, and crop parameters, and accounting for time-varying field conditions that include timing and amount of irrigation, variable soil salinity conditions, and variable irrigation water quality including rainfall. Particularly, the HYDRUS software packages (Šimůnek et al., 2016) have the capability of evaluating salt transport in the soil profile using several modeling concepts. The standard solute transport module in HYDRUS considers the transport of one or multiple solutes, which can be either independent or involved in sequential first-order decay reactions (Hanson et al., 2008; Forkutsa et al., 2009; Roberts et al., 2009; Ramos et al., 2012). The major ion chemistry module adapted from the UNSATCHEM model (Šimůnek et al., 2016) allows for the simulation of multicomponent solute transport, describing the subsurface transport of multiple ions that may mutually interact, create various complex species, compete for sorption sites, and/or precipitate or dissolve (Gonçalves et al., 2006; Ramos et al., 2011; Rasouli et al., 2013; Rajj et al., 2016). Finally, the HPx module (Jacques et al., 2018), in contrast to the previous module which is constrained to specific elements, offers users the flexibility to simulate multicomponent solute transport while defining their own species with particular chemical properties and reactions. However, to the best of our knowledge, no applications related to salinity problems have been yet reported using HPx.

Two of the approaches described above were already used to simulate solute transport in the Alentejo region, thus providing the necessary support for this study. Gonçalves et al. (2006) successfully simulated soil water contents, concentrations of major cations (Na^+ , Ca^{2+} , Mg^{2+}), the electrical conductivity of the soil solution (EC_{sw}), the sodium adsorption ratio (SAR), and the percentage of exchangeable sodium (ESP) in 3 field lysimeters irrigated with waters of different quality for 4 years using the major chemistry module of the HYDRUS-1D model (Šimůnek et al., 2016). Later, Ramos et al. (2011, 2012) demonstrated the fundamentals of the multicomponent transport modeling approach in terms of model outputs, revealing that EC_{sw} can be adequately simulated as a nonreactive tracer in the absence of processes of precipitation/dissolution in the soil profile, while the major cations and SAR can only be successfully simulated when considering interactions between species and the competition for sorption sites.

The overall objective of this study thus is to evaluate the long-term impact of irrigation practices carried out in very high-density olive orchards grown in the Alentejo region using a multicomponent transport modeling approach. This study makes use of the existing knowledge on local soil and water resources, the capability of the major chemistry module of the HYDRUS-1D model (Šimůnek et al., 2016) to accurately describe soil salinization and sodification in the soil profile, and the work already carried out in the region in calibrating/validating HYDRUS-1D. The specific objectives are then (i) to define baseline levels of soil salinity/sodicity based on surveys carried out in the region before the expansion of olive orchards and (ii) to simulate long-term (30 years) soil salinization and sodification risks in different soil profiles using eight different scenarios. The irrigation scenarios include current monitored irrigation practices, using irrigation waters with different quality, planting maize as an alternative crop, and considering climate change projections for the region. Limitations related to the modeling approach and future research needs are also addressed. These include the need for field measured datasets for calibrating/validating modelling applications, namely those that use more realistic representations of the soil domain and irrigation system adopted here. Nonetheless, this work demonstrates how the state-of-the-art knowledge can be combined without great cost to assess the long-term sustainability of production systems.

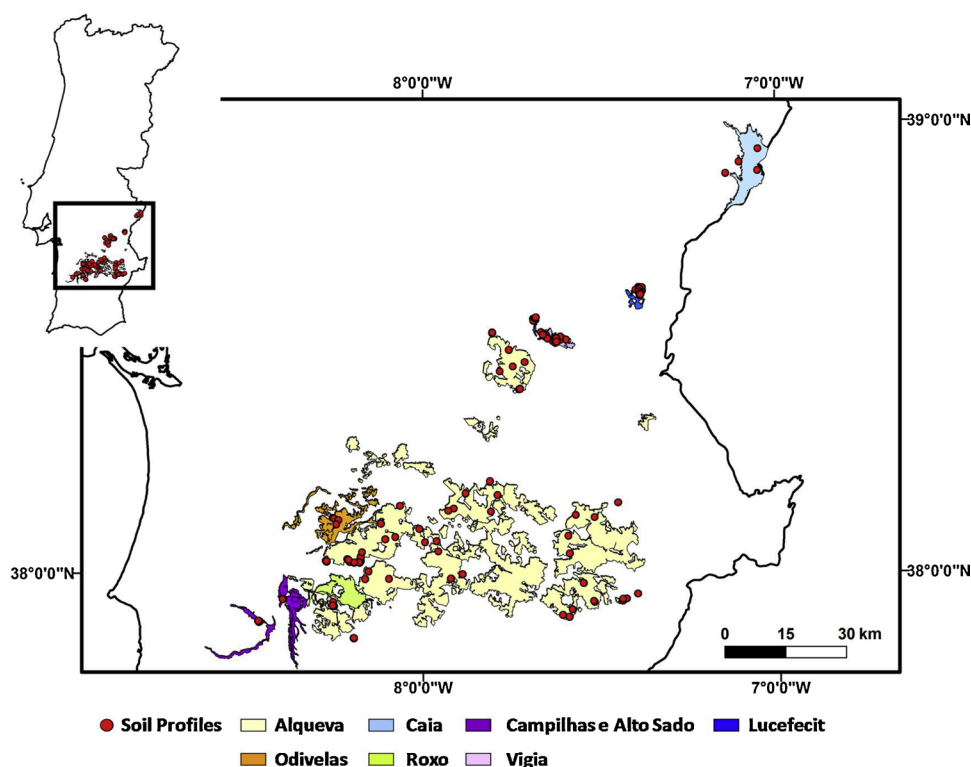


Fig. 1. Location of soil profiles and irrigation districts.

2. Material and methods

2.1. Study site description

This study was carried out in some of the main irrigated areas of the Alentejo region, southern Portugal (Fig. 1), which included Alqueva (110,000 ha), Caia (7237 ha), Campilhas e Alto Sado (5555 ha), Lucefecit (1175 ha), Odivelas (6846 ha), Roxo (5041 ha), and Vigia (1500 ha). The climate in the region is semi-arid to dry sub-humid, with hot dry summers and mild winters with irregular rainfall. The mean annual temperature is 15.5 °C (1979–2009), with daily surface air temperatures at the coolest (January) and warmest (July) months averaging 8.1 and 23.4 °C, respectively, while the minimum and maximum daily averages reach -2.9 and 33.1 °C, respectively. The mean annual rainfall is 385 mm (1979–2009), mostly occurring between September and May, but also showing a strong annual variability with annual values ranging between 178 and 816 mm (Fig. 2). The mean annual reference evapotranspiration (ET_0) is 989 mm (1979–2009), varying between 908 and 1066 mm, while daily ET_0 rates average between 0.6 mm d⁻¹ in December and 5.6 mm d⁻¹ in July (Fig. 2). The soils in the region are predominantly classified as Luvisols (47.0%), Vertisols (20.2%), Calcisols (13.4%), Fluvisols (9.5%), and Cambisols (5.7%) (IUSS Working Group WRB, 2014). For many decades, the main irrigated crops were maize (*Zea mays* L.), tomato (*Solanum lycopersicum* L.), rice (*Oryza sativa* L.), and sunflower (*Helianthus annuus* L.). Recently, olive trees have become the main land use in the region, with olive orchards now covering 42,040 ha in Alqueva, 4149 ha in Caia, 1498 ha in Campilhas e Alto Sado, 123 ha in Lucefecit, 5033 ha in Odivelas, 3138 ha in Roxo, and 942 ha in Vigia (DGADR, 2018).

2.2. Simulated scenarios

Soil salinization and sodification risks were assessed for eight different scenarios (S), which considered current irrigation practices monitored in very-high density olive orchards grown in the Alentejo region (S1), different qualities of irrigation waters (S2–S6), maize as an

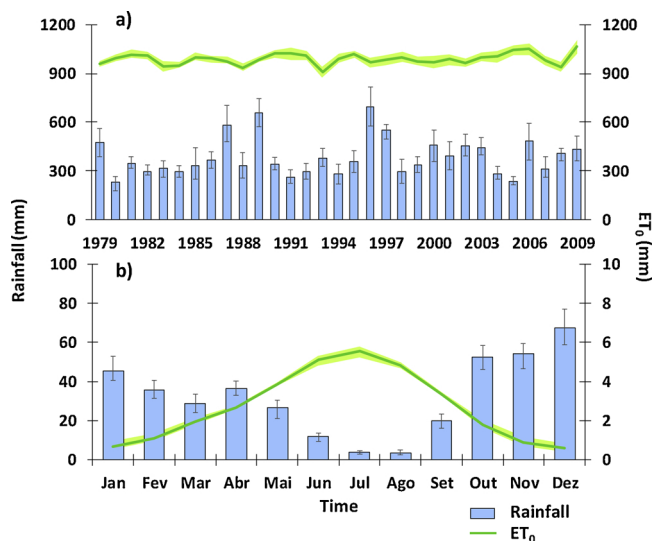


Fig. 2. Average yearly (a) and monthly (b) values of rainfall and reference evapotranspiration (ET_0) for the period 1979–2009 (vertical bars and shaded area represent maximum and minimum values).

alternative crop (S7), and climate change projections for the region (S8). Scenarios were run for a 30-year period and 160 soil profiles.

The current monitored irrigation practices scenario (S1) was defined according to Paço et al. (2014) and Darouich et al. (private communication), who quantified evapotranspiration rates and crop coefficients for very-high density olive orchards (1.35 m × 3.75 m; 975 trees ha⁻¹) in commercial farms in the Alentejo region for five years. Monitored annual irrigation amounts varied between 287 and 446 mm, with water being applied almost every day during spring and summer at an average depth of 3 mm per event using a drip system. Hence, the S1 scenario assumed these observations as a standard irrigation practice in the region, with total irrigation being set to 324 mm y⁻¹, applied

Table 1
Irrigation depths and ionic composition of irrigation waters applied in each scenario (values in brackets correspond to the standard deviation of measured values).

Scenario	Irrigation		Ionic composition of irrigation waters							Reference	
	(mm year ⁻¹)	(mm event ⁻¹)	EC _{iw} (dS m ⁻¹)	Ca ²⁺ (mmolc L ⁻¹)	Mg ²⁺	K ⁺	Na ⁺	Cl ^{-b}	SAR (mmolc L ⁻¹) ^{0.5}		USSL classification ^c
1	324	3	0.52 (0.05) ^a	1.76 (0.16)	1.64 (0.07)	0.14 (0.02)	1.63 (0.32)	5.17 (0.46)	1.25 (0.24)	C2S1	EDIA (2018)
2	324	3	0.81	1.85	3.65	0.14	2.50	8.14	1.51	C3S1	Gonçalves et al. (2006)
3	324	3	1.01	2.80	3.00	0.14	4.16	10.10	2.44	C3S1	Ramos et al. (2011)
4	324	3	1.61	3.16	6.32	0.14	6.52	16.14	2.99	C3S1	Gonçalves et al. (2006)
5	324	3	1.61	1.93	3.86	0.14	10.21	16.14	6.00	C3S2	Ramos et al. (2011)
6	324	3	3.21	5.10	10.20	0.14	16.70	32.14	6.04	C4S2	Gonçalves et al. (2006)
7	500	10	0.52	1.76	1.64	0.14	1.63	5.17	1.25	C2S1	EDIA (2018)
8	324	3	0.52	1.76	1.64	0.14	1.63	5.17	1.25	C2S1	EDIA (2018)

EC_{iw}, electrical conductivity of the irrigation water; SAR, sodium adsorption ratio.

^a values in brackets correspond to the standard deviation of the measured values.

^b calculated to maintain the charge balance.

^c U.S. Salinity Laboratory Staff (1954). C2, medium-salinity water (EC_{iw} 0.25–0.75 dS m⁻¹); C3, high-salinity water (EC_{iw} 0.75–2.25 dS m⁻¹); C4, very high salinity water (EC_{iw} > 2.25 dS m⁻¹); S1, low-sodium water (SAR limits depend on EC_{iw}); S2, medium-sodium water (SAR limits depend on EC_{iw}).

almost every day from mid-May to mid-October, and also with an average depth of 3 mm per event (27 mm in May; 45 mm in June; 93 mm in July; 93 mm in August; 45 mm in September; and 21 mm in October). These values are different from those reported by [Cameira et al. \(2014\)](#) and [Conceição et al. \(2017\)](#) for deficit irrigated high-density orchards (7.0 m × 4.8 m; 300 trees ha⁻¹), where seasonal irrigation reached only 141 to 226 mm (1.3 to 1.7 mm per event). In S1, the same irrigation scheduling was adopted throughout the years since the objective was to quantify the long-term salt accumulation in the soil profile and not to meet crop water requirements. The S1 scenario further considered the quality of irrigation waters monitored at 14 different locations in Alqueva between May and June 2017 ([EDIA, 2018](#)). The mean values of the measured electrical conductivity of irrigation waters (EC_{iw}), concentrations of major cations, and SAR are presented in [Table 1](#).

The S2 to S6 scenarios considered the same standard irrigation practice as in S1 but with lower water quality as in [Gonçalves et al. \(2006\)](#) and [Ramos et al. \(2011\)](#) ([Table 1](#)). Water quality in the S2 through S5 scenarios was thus based on values monitored in the region over the years (wherein EC_{iw} has frequently reached values of 0.8–2.4 dS m⁻¹) while S6 considered extreme conditions that are hardly observed in Alentejo.

The S7 scenario considered maize, another traditional crop in the region, as an alternative crop to olive. Irrigation was defined according to [Ramos et al. \(2011, 2017a\)](#), with water being applied between mid-May and mid-September, with a total of 500 mm per season and 10 mm per event (30 mm in May; 120 mm in June; 150 mm in July; 150 mm in August; and 50 mm in September). Water quality was set as in S1 ([Table 1](#)).

The S8 scenario considered climate change projections by the Portuguese Local Warming Website Project (<https://portaldoclima.pt/en/>) for the Alentejo region. This project made available projections of climate variables down to local administrative regions (NUTS3) at a monthly and seasonal scales based on simulations provided by an ensemble of state-of-the-art regional climate models forced by five global climate models. Here, S8 adopted the Representative Concentration Pathway 4.5 (RCP4.5) scenario for greenhouse emissions ([Stocker et al., 2013](#)), with the average surface air temperature in the region expected to increase 0.8 °C while annual rainfall to decrease 20–30 mm for the period 2011–2040. RCP4.5 represents one intermediate stabilization pathway, in which radiative forcing is stabilized at approximately 4.5 W m⁻² after 2100 (assuming then constant greenhouse gases and aerosols concentrations in the atmosphere after 2150) ([Stocker et al., 2013](#)). Additional (more extreme) scenarios also available from the same Project were not considered here as the objective was not to conduct an extensive analysis on the impacts of climate change on soil salinization and sodification but to provide an insight on possible trends. Nonetheless, the climate variability in the region was considered to provide sufficient information on possible outcomes for the worse case projections. In S8, the irrigation scheduling and the quality of irrigation waters were set as in S1 ([Table 1](#)).

2.3. Modeling approach

The HYDRUS-1D software package version 4.16 ([Šimůnek et al., 2016](#)) was used to numerically simulate one-dimensional water flow and solute transport in variably-saturated porous media by solving the Richards and Fickian-based convection–dispersion (CDE) equations, respectively. The flow equation considered the analytical models proposed by [Mualem \(1976\)](#) and [van Genuchten \(1980\)](#) for describing soil hydraulic properties, in which six parameters are required, i.e., the residual (θ_r) and saturated (θ_s) water contents, the saturated hydraulic conductivity (K_s), the connectivity/tortuosity factor (λ), and two shape parameters (α and η). The flow equation further incorporated a sink term to account for root water uptake by plants. The macroscopic approach introduced by [Feddes et al. \(1978\)](#) was then considered, where

the potential root water uptake rate, corresponding to the potential transpiration rate (T_p), was distributed over the root zone and reduced due to by the presence of depth-varying water and salinity stresses (Skaggs et al., 2006; Šimůnek and Hopmans, 2009). The water stress response function was defined according to Feddes et al. (1978), in which root water uptake is at the potential rate when the pressure head (h) is between h_2 and h_3 , drops off linearly when $h > h_2$ or $h < h_3$, and becomes zero when $h < h_4$ or $h > h_1$ (subscripts 1–4 denote different threshold pressure heads). The salinity stress response function was defined according to Maas (1990), which is implemented in the major ion chemistry module of HYDRUS-1D in terms of the osmotic head (h_ϕ). This stress response function requires two parameters, i.e., the osmotic head threshold value ($h_{\phi T}$) corresponding to the value of h_ϕ above which root water uptake occurs without a reduction and the slope (s) which determines the root water uptake decline per a unit decrease in the osmotic head below the threshold. The effects of the water and salinity stresses were further assumed to be multiplicative (van Genuchten, 1987), enhancing those effects on root water uptake (Oster et al., 2012).

The major ion chemistry module of HYDRUS-1D took into account the fact that the soil liquid phase always contains a mixture of many ions that may interact, create complex species, precipitate, dissolve, and/or compete for sorption sites on the solid phase (Šimůnek et al., 2014). The numerical model thus considered all these interactions, including aqueous complexation, precipitation/dissolution, and cation exchange. The partition of solutes between the liquid and solid phases was described using the Gapon exchange equation (White and Zelazny, 1986), further assuming that the cation exchange capacity (CEC) was constant, given by the sum of the exchangeable cations (Ca^{2+} , Mg^{2+} , Na^+ , and K^+), and independent of pH. Precipitation/dissolution reactions considered multicomponent kinetic expressions, which included both forward and back reactions. The Pitzer expressions were adopted for computing single ion activities (Šimůnek et al., 2013). The electrical conductivity of the soil solution (EC_{sw}) was determined from individual anions and cations following McNeal et al. (1970), while the sodium adsorption ratio (SAR) was computed from the simulated soluble Na^+ , Ca^{2+} , Mg^{2+} concentrations according to the U.S. Salinity Laboratory Staff (1954) guidelines.

2.4. Model setup

Various scenarios were run for 160 selected soil profiles for a 30-year period using the major ion chemistry module of the HYDRUS-1D software package. The upper boundary condition was determined by the potential evaporation and transpiration rates, and the irrigation, rainfall, and concentration fluxes (Fig. 2; Table 1). The bottom boundary condition was specified as free drainage based on groundwater levels monitored by the Portuguese Environmental Agency in 79 piezometric stations located in the region between 1997 and 2018 (SNIRH, 2018). The groundwater table was reported to be on average at a depth of 5.5 m while its maximum and minimum levels averaged at depths of 7.6 and 4.2 m, respectively.

Soil information was extracted from the INFOSOLO (Ramos et al., 2017b) and PROPSOLO (Gonçalves et al., 2011) databases. The former is a soil information system developed to compile soil data produced in Portugal (the soil legacy database) and to support stakeholders and land managers in the decision-making. The latter was specifically developed to store soil hydraulic properties and for developing soil pedotransfer functions (PTFs) that indirectly estimate them from basic soil properties (Ramos et al., 2013, 2014a, 2014b). 160 soil profiles located in the study area (Fig. 1) with a complete description of soil physical (Table 2) and chemical (Table 3) properties of different soil horizons/layers were selected for running the scenarios described above. The soil profiles included a variety of Luvisols (63), Fluvisols (40), Vertisols (27), Calcisols (15), Regosols (11), and Cambisols (4) (IUSS Working Group WRB, 2014). The soil profiles were defined to be 1.5 m deep, having 2

to 6 layers according to available observations. The physical and chemical characteristics of the deepest observed soil layer were extended to the bottom of the soil profile when necessary. Initial soil water contents were always set to a uniform value of $0.25 \text{ cm}^3 \text{ cm}^{-3}$. The initial conditions for the major ion chemistry module were given for each horizon/layer in terms of concentrations of Na^+ , Ca^{2+} , Mg^{2+} , and K^+ in the liquid and solid phases. The soil hydraulic parameters of the Mualem-van Genuchten model (Mualem, 1976; van Genuchten, 1980) were taken from the PROPSOLO database, complemented with PTFs of Ramos et al. (2014b) for the characterization of deeper soil layers (24% of the data) or the hydraulic conductivity curve (K_s and λ in 42% of the data). Solute transport parameters were estimated from PTFs proposed by Gonçalves et al. (2002). The Gapon exchange constants were taken from Ramos et al. (2011) and were interpreted as follows: for the Ca^{2+}/Mg^{2+} exchange ($K_{Ca/Mg} = 0.35$), Mg^{2+} was the preferred ion relative to Ca^{2+} on the exchange complex. For the Ca^{2+}/Na^+ exchange ($K_{Ca/Na} = 2.90$), Ca^{2+} was the preferred ion relative to Na^+ . Finally, for the Ca^{2+}/K^+ exchange ($K_{Ca/K} = 0.11$), K^+ was the preferred ion relative to Ca^{2+} (Mallants et al., 2017).

Simulations were run using a climate dataset from 1979–2009. The weather variables (rainfall (mm), average surface air temperature ($^{\circ}C$), wind speed (m s^{-1}), relative humidity (%), and solar radiation (W m^{-2})) were provided for the study area by the MM5 mesoscale model (<http://meteo.tecnico.ulisboa.pt>), forced by the initial conditions from the NCEP (National Centers for Environmental Prediction) Climate Forecast System Reanalysis, at a spatial resolution of 9 km. These data were then used to compute daily reference evapotranspiration (ET_0) rates with the FAO Penman-Monteith method (Allen et al., 1998). The S1 to S7 scenarios assumed the same climate conditions of 1979–2009, while the S8 scenario considered a $0.8^{\circ}C$ increase in the mean surface air temperature as well as a 30 mm decrease in the mean annual rainfall values following projections from the Portuguese Local Warming Website Project (<https://portaldoclima.pt/en/>). Hence, mean surface air temperature anomalies were projected on the 1979–2009 dataset by increasing daily temperatures by $0.8^{\circ}C$, while rainfall reductions were considered between April and October, also taking into account the projected rainfall increase during the remaining months.

Crop evapotranspiration (ET_c) values were computed from daily ET_0 rates using the single crop coefficient (K_c) approach (Allen et al., 1998). For olive (S1–S6, S8), K_c values between 0.53 and 0.83 were adopted for different months of the year as reported by Paço et al. (2014) and Darouich et al. (private communication). A ground cover of 0.35 (Paço et al., 2014) was also considered for estimating the leaf area index (LAI) of olive orchards following Allen and Pereira (2009). That value was then used for the partition of the ET_c values into T_p and soil evaporation (E_p) rates according to Ritchie (1972). For maize (S7), K_c values of 0.30, 1.20, and 0.35 were considered for the initial, mid-season, and late season crop stages, respectively, with these values corresponding to the standard K_c values for the Mediterranean region (Allen et al., 1998). The simulated LAI curve from Ramos et al. (2017a) was then used for the partition of maize ET_c values into T_p and E_p rates (Ritchie, 1972). Those authors calibrated/validated a crop growth model for simulating the LAI curve and other crop state variables as a function of the heat units, solar radiation, crop stress, and the crop development stage using measured data collected in the Sorraia Valey region, southern Portugal.

For olive, T_p reductions due to the water stress were computed with the following parameters: $h_1 = -10 \text{ cm}$, $h_2 = -25 \text{ cm}$, $h_3 = -3000$ to -5000 cm , $h_4 = -18,000 \text{ cm}$. These values were taken from Egea et al. (2016), who parameterized the Feddes et al. (1978) model for this crop based on a literature review on the relationship between the maximum stomatal conductance and predawn leaf water potential. T_p reductions due to the salinity stress considered olive as a moderately tolerant crop to soil salinity (Ayers and Westcot, 1985; Maas and Hoffman, 1977), with the following parameters being adopted: $h_{\phi T} = -2975 \text{ cm}$ and $s = 0.00021$. These values were defined based on threshold values for the electrical conductivity of the soil saturation extract (EC_e), being first

Table 2
Main physical soil characteristics (values in brackets correspond to the standard deviation of measured values).

Soil/layer	Layer top (cm)	Layer bottom (cm)	Coarse sand (%)	Fine sand (%)	Silt (%)	Clay (%)	Bulk density (g cm ⁻³)	θ _t (cm ³ cm ⁻³)	θ _s (cm ³ cm ⁻³)	α (cm ⁻¹)	η (°)	K _s (cm d ⁻¹)	λ (°)	D _L (cm)
Calcisols														
1	0(0)	33(10)	20.9(7.4)	25.5(5.6)	15.5(4.8)	38.0(10.3)	1.40(0.13)	0.095(0.068)	0.530(0.051)	0.176(0.120)	1.188(0.082)	156.8(172.2)	-5.77(2.38)	4.7(3.7)
2	28(11)	45(11)	16.5(7.0)	17.2(1.8)	17.4(9.7)	48.9(6.7)	1.36(0.04)	0.074(0.032)	0.496(0.010)	0.060(0.035)	1.119(0.023)	66.1(13.3)	-7.64(0.46)	3.3(1.9)
≥ 3	63(12)	88(15)	26.2(3.2)	12.4(1.1)	11.7(2.5)	49.8(0.7)	1.38(0.04)	0.074(0.019)	0.416(0.08)	0.083(0.014)	1.756(0.301)	95.0(24.9)	-0.86(3.04)	7.9(0.5)
Cambisols														
1	0(0)	26(8)	41.5(7.2)	35.0(6.5)	9.2(1.5)	14.3(2.4)	1.62(0.07)	0.041(0.026)	0.411(0.029)	0.066(0.022)	1.246(0.059)	36.1(13.5)	-4.16(1.24)	5.3(1.9)
2	28(8)	50(12)	35.4(7.5)	31.3(8.5)	9.8(1.9)	23.5(11.9)	1.67(0.07)	0.031(0.007)	0.398(0.061)	0.087(0.096)	1.157(0.034)	16.9(5.8)	-6.38(1.83)	7.1(6.8)
≥ 3	66(30)	97(36)	41.5(8.8)	27.0(3.9)	8.3(2.6)	23.2(6.6)	1.70(0.10)	0.059(0.026)	0.377(0.027)	0.105(0.066)	1.195(0.057)	41.3(21.3)	-5.03(1.63)	10.5(6.1)
Fluvisols														
1	4(5)	22(11)	10.1(7.0)	50.5(5.9)	26.1(2.7)	13.2(1.4)	1.52(0.10)	0.038(0.021)	0.390(0.031)	0.023(0.031)	1.278(0.056)	33.4(45.7)	-4.60(1.13)	2.7(0.9)
2	30(12)	57(19)	15.8(12.0)	40.3(9.1)	25.7(5.2)	18.2(6.4)	1.56(0.12)	0.053(0.037)	0.386(0.032)	0.054(0.045)	1.230(0.071)	59.1(53.1)	-5.11(1.81)	5.3(4.5)
≥ 3	62(23)	106(35)	13.7(10.5)	39.1(9.4)	26.2(4.6)	21.1(7.4)	1.64(0.14)	0.061(0.034)	0.389(0.042)	0.077(0.067)	1.199(0.071)	78.2(90.2)	-6.11(1.90)	6.1(5.3)
Luvisols														
1	0(0)	27(7)	33.3(10.6)	35.4(8.9)	12.6(4.6)	18.7(9.7)	1.62(0.12)	0.054(0.035)	0.392(0.050)	0.122(0.121)	1.240(0.129)	78.4(86.1)	-4.16(2.21)	5.4(5.4)
2	27(7)	55(14)	29.5(11.4)	29.6(7.6)	12.7(4.5)	28.3(11.3)	1.66(0.12)	0.077(0.038)	0.387(0.059)	0.098(0.103)	1.169(0.078)	40.0(51.1)	-5.81(2.57)	6.2(5.8)
≥ 3	77(29)	113(34)	37.0(17.9)	25.8(8.7)	12.3(6.6)	24.9(10.5)	1.68(0.11)	0.070(0.026)	0.406(0.033)	0.076(0.026)	1.221(0.093)	61.8(47.6)	-5.02(1.84)	6.8(2.9)
Regosols														
1	0(0)	22(9)	27.8(7.0)	29.0(6.5)	27.4(9.4)	15.8(6.6)	1.52(0.10)	0.049(0.028)	0.412(0.059)	0.190(0.383)	1.253(0.103)	68.6(63.0)	-6.25(2.70)	10.9(18.9)
2	24(11)	52(20)	25.3(10.0)	28.1(4.7)	29.1(10.8)	17.5(8.1)	1.60(0.07)	0.058(0.032)	0.388(0.036)	0.037(0.044)	1.307(0.129)	30.7(23.8)	-5.26(1.21)	3.8(2.1)
≥ 3	87(17)	154(26)	27.1(3.4)	18.3(4.4)	21.5(5.6)	33.2(13.4)	1.56(0.01)	0.085(0.024)	0.438(0.014)	0.068(0.030)	1.148(0.048)	43.3(0.4)	-7.09(0.59)	6.7(3.2)
Vertisols														
1	0(0)	30(9)	17.2(9.1)	25.8(5.8)	17.3(5.1)	39.7(10.0)	1.46(0.18)	0.088(0.049)	0.498(0.059)	0.196(0.161)	1.136(0.063)	90.9(76.2)	-7.31(1.98)	7.6(6.4)
2	28(6)	62(13)	14.0(6.3)	24.7(6.2)	16.9(3.4)	44.4(9.3)	1.52(0.15)	0.122(0.051)	0.483(0.060)	0.085(0.062)	1.150(0.057)	44.6(40.3)	-6.99(2.94)	4.4(3.1)
≥ 3	82(24)	130(19)	34.2(25.8)	22.8(8.4)	12.2(8.8)	30.8(18.5)	1.57(0.09)	0.076(0.031)	0.437(0.050)	0.091(0.031)	1.249(0.180)	108.2(86.3)	-5.18(2.27)	7.7(2.3)

θ_r, residual water content; θ_s, saturated water content; α and η, empirical shape parameters; λ_s, pore connectivity/tortuosity parameter; K_s, saturated hydraulic conductivity; D_L, longitudinal dispersivity.

Table 3
Main chemical soil characteristics (values in brackets correspond to the standard deviation of measured values).

Soil/layer	OM (%)	pH (·)	EC _e (dS m ⁻¹)	Soluble ions (mmol _e L ⁻¹)				SAR (mmol _e L ⁻¹) ^{0.5}				Exchangeable cations (mmol _e kg ⁻¹)			CEC (mmol _e kg ⁻¹)	ESP (%)
				Ca ²⁺	Mg ²⁺	K ⁺	Na ⁺	Cl ⁻	Ca ²⁺	Mg ²⁺	K ⁺	Na ⁺	Ca ²⁺	Mg ²⁺		
Calcisols																
1	1.9(0.5)	8.44(0.16)	0.33(0.09)	1.36(0.44)	0.09(0.04)	0.05(0.05)	0.21(0.26)	1.70(0.67)	0.34(0.37)	304.1(99.7)	8.0(3.2)	2.5(2.1)	0.7(0.4)	315.3(100.8)	0.21(0.15)	
2	1.2(0.1)	8.43(0.20)	0.29(0.01)	1.53(0.33)	0.11(0.03)	0.03(0.03)	0.13(0.01)	1.80(0.40)	0.17(0.01)	282.2(8.4)	8.9(0.3)	2.1(1.5)	0.4(0.1)	293.6(6.6)	0.14(0.03)	
≥ 3	0.6(0.1)	8.68(0.07)	0.29(0.05)	1.33(0.27)	0.10(0.03)	0.04(0.01)	0.15(0.01)	1.62(0.07)	0.23(0.02)	183.3(31.4)	9.6(5.7)	2.5(0.6)	0.7(0.3)	196.1(36.7)	0.38(0.10)	
Cambisols																
1	0.7(0.2)	7.28(0.27)	0.54(0.64)	0.42(0.44)	0.29(0.27)	0.03(0.02)	0.68(0.80)	1.41(1.51)	1.59(1.35)	103.7(44.8)	35.9(16.6)	1.1(0.6)	1.2(0.7)	141.9(58.3)	0.60(0.36)	
2	0.5(0.1)	7.47(0.48)	0.47(0.52)	0.26(0.23)	0.20(0.16)	0.01(0.00)	0.94(0.82)	1.41(1.18)	2.72(1.84)	122.6(30.0)	65.2(41.3)	0.9(0.4)	3.9(3.6)	192.6(70.0)	1.42(0.97)	
≥ 3	0.2(0.2)	8.83(0.33)	1.69(0.56)	0.84(0.43)	0.72(0.27)	0.01(0.00)	4.52(1.75)	6.09(2.32)	7.52(1.36)	113.8(25.8)	68.8(39.6)	1.1(0.3)	14.2(7.1)	197.8(68.0)	5.92(2.10)	
Fluvisols																
1	1.9(0.8)	6.28(0.87)	0.70(0.98)	1.66(2.71)	1.10(1.66)	0.06(0.02)	1.81(1.92)	4.63(6.25)	3.07(2.71)	53.1(21.0)	23.9(8.7)	2.3(1.6)	4.9(3.9)	88.8(29.6)	4.14(3.88)	
2	0.6(0.2)	6.45(0.99)	0.74(0.73)	0.83(0.50)	0.78(0.50)	0.02(0.01)	2.84(2.41)	4.47(3.35)	4.22(2.72)	63.1(26.4)	39.0(23.6)	1.5(0.7)	8.4(7.5)	116.5(49.8)	4.59(3.63)	
≥ 3	0.5(0.4)	6.98(1.06)	0.94(1.03)	1.30(1.20)	1.41(1.34)	0.02(0.01)	4.67(4.23)	7.38(6.67)	5.09(3.19)	102.4(59.5)	51.9(31.2)	0.9(0.5)	15.4(12.9)	178.0(98.1)	6.38(4.44)	
Luvissols																
1	1.3(0.6)	6.81(0.93)	0.73(0.94)	0.86(1.08)	0.42(0.56)	0.08(0.15)	0.90(1.12)	2.25(2.60)	2.09(1.58)	83.4(56.0)	30.7(32.7)	1.8(2.3)	2.6(3.1)	120.9(74.0)	2.05(3.36)	
2	0.5(0.4)	7.16(0.68)	0.67(1.09)	0.85(1.23)	0.44(0.74)	0.02(0.03)	1.39(1.80)	2.71(3.49)	2.69(2.13)	139.3(69.1)	62.4(42.5)	1.3(1.2)	5.8(7.1)	211.4(98.2)	2.80(3.79)	
≥ 3	0.5(0.4)	7.65(0.89)	1.25(1.33)	0.93(0.93)	0.76(0.93)	0.02(0.03)	3.54(3.75)	5.25(5.29)	5.53(4.27)	132.5(70.8)	63.7(35.6)	0.9(0.6)	11.0(10.0)	213.4(85.5)	4.96(4.31)	
Regosols																
1	1.6(0.6)	6.52(1.29)	0.77(0.32)	1.22(0.51)	0.77(0.18)	0.02(0.01)	0.94(0.61)	2.94(1.29)	1.29(0.62)	88.5(76.7)	26.8(18.7)	3.9(4.2)	4.4(2.8)	123.7(93.2)	5.03(3.18)	
2	1.1(0.4)	6.69(0.86)	1.04(0.00)	2.55(0.00)	0.76(0.00)	0.02(0.00)	1.47(0.00)	4.80(0.00)	1.49(0.00)	74.7(78.5)	24.7(11.0)	0.9(0.2)	2.9(0.5)	103.1(88.7)	3.44(1.58)	
≥ 3	0.4(0.2)	7.84(1.00)	0.54(0.11)	1.31(0.52)	0.72(0.05)	0.04(0.03)	0.67(0.35)	2.73(0.10)	0.85(0.49)	156.0(84.2)	69.6(36.0)	0.8(0.3)	2.5(0.8)	228.8(109.5)	1.52(1.05)	
Vertisols																
1	1.6(0.6)	7.82(0.56)	0.58(0.42)	2.04(2.33)	0.36(0.29)	0.02(0.02)	0.58(0.63)	3.00(10.36)	0.89(0.98)	270.4(85.9)	41.7(25.1)	1.7(1.5)	2.5(1.5)	316.3(89.3)	0.81(0.61)	
2	1.3(0.6)	7.81(0.58)	0.54(0.56)	1.82(1.82)	0.52(0.75)	0.02(0.01)	0.37(0.28)	2.73(4.13)	0.54(0.36)	250.5(76.0)	50.7(27.7)	1.3(1.2)	3.1(2.9)	305.6(83.8)	1.09(1.24)	
≥ 3	0.5(0.3)	8.38(0.47)	0.52(0.27)	1.09(0.90)	0.46(0.28)	0.01(0.01)	0.93(1.30)	2.49(21.25)	1.63(2.02)	193.7(70.0)	72.5(48.5)	0.9(0.6)	5.3(7.5)	272.4(98.9)	1.81(2.51)	

OM, organic matter content; EC_e, electrical conductivity of the saturation extract; SAR, sodium adsorption ratio; CEC, cation exchange capacity; ESP, exchangeable sodium percentage.

converted into EC_{sw} using the $EC_{sw}/EC_e = 2$ ratio, and later into h_{ϕ} using a linear relationship found by U.S. Salinity Laboratory Staff (1954). For maize, the water stress was computed with the following parameters: $h_1 = -15$ cm, $h_2 = -30$ cm, $h_3 = -325$ to -600 cm, $h_4 = -8000$ cm (Wesseling et al., 1991). T_p reductions due to the salinity stress were obtained by setting $h_{\phi T} = -1244.88$ cm and $s = 0.000157456$ (Ayers and Westcot, 1985; Ramos et al., 2011).

In Olive, the root depth was set to 1.2 m in all soil profiles (Paço et al., 2014; Darouich et al., private communication), except for Calcisols where it was constrained by the depth of the calcareous layer located below 0.31–1.08 m. In maize, the root depth was set to 0.6 m (Ramos et al., 2011), with the same constraints for Calcisols.

3. Results and discussion

3.1. Baseline salinity and sodicity levels

Calcisols (15 soil profiles) selected for this study were mostly located in Alqueva (Brinches, Brinches-Enxoé, Orada-Amoreira, and Ervidel irrigation blocks) and Vigia. Olive orchards already covered 80% of the area when the soil profiles were characterized. The measured EC_e values of the topsoil layers averaged 0.33 dS m^{-1} (Table 3), ranging from 0.23 to 0.52 dS m^{-1} , while the bottom layers averaged 0.29 dS m^{-1} , varying from 0.25 to 0.36 dS m^{-1} . As such, the measured salinity levels were relatively low and smaller than the threshold limit ($< 1.3 \text{ dS m}^{-1}$) defined by Ayers and Westcot (1985) for crops sensitive to soil salinity. Likewise, the SAR values computed from Na^+ , Ca^{2+} , and Mg^{2+} concentrations measured in the soil solution (hereafter denoted as measured SAR values) were also relatively low, averaging $0.34 \text{ (mmol}_c \text{ L}^{-1})^{0.5}$ in the topsoil layer (ranging from 0.11 to $1.33 \text{ (mmol}_c \text{ L}^{-1})^{0.5}$) and decreasing then with depth.

Cambisols (4 soil profiles), being less represented in the study area, were located in Alqueva (Ervidel, Serpa, and Monte Novo). Olive orchards were the dominant land use at all sites. The measured EC_e values of the topsoil layers averaged 0.54 dS m^{-1} (Table 3), showing relatively large variations (0.10 – 1.64 dS m^{-1}) that were also visible at deeper depths. The same variability was further noticed in the measured SAR values, with the topsoil layer average reaching $1.59 \text{ (mmol}_c \text{ L}^{-1})^{0.5}$, while the maximum and minimum values were 3.90 and $0.62 \text{ (mmol}_c \text{ L}^{-1})^{0.5}$, respectively. Two soil profiles showed evidence of salt accumulation in the deeper layers, with measured EC_e values reaching 0.91 – 1.52 dS m^{-1} below the 50 cm depth (SAR between 5.73–7.80 $\text{(mmol}_c \text{ L}^{-1})^{0.5}$) and 1.87 – 2.47 dS m^{-1} below the 100 cm depth (SAR $> 9.0 \text{ (mmol}_c \text{ L}^{-1})^{0.5}$). These values may well have resulted from irrigation and fertilization management practices or the characteristics of the parent material (igneous rocks and consolidated clastic sedimentary rocks) since no detailed information regarding historical management practices or the characteristics of the parent material existed. Nonetheless, the measured salinity levels ($< 3.0 \text{ dS m}^{-1}$) found in these locations were well tolerable by crops moderately sensitive to soil salinity (Ayers and Westcot, 1985).

Fluvisols (40 soil profiles) were mainly distributed in Campilhas e Alto Sado, but also in Alqueva (Odivelas Fase II). The main land uses were maize, wheat (*Triticum aestivum* L.), sugar beet (*Beta vulgaris* L.), pasture, and fallow. For the topsoil layers, the measured EC_e and SAR values averaged 0.33 dS m^{-1} and $3.07 \text{ (mmol}_c \text{ L}^{-1})^{0.5}$ (Table 3), respectively, ranging from 0.20 to 3.59 dS m^{-1} and from 0.76 to $5.96 \text{ (mmol}_c \text{ L}^{-1})^{0.5}$, respectively. For the bottom layers and at different depths, the measured EC_e values reached averages of 0.74 – 0.94 dS m^{-1} (ranging from 0.23 to 3.99 dS m^{-1}) while the measured SAR values averaged 4.22 – $5.09 \text{ (mmol}_c \text{ L}^{-1})^{0.5}$ (ranging from 1.26 to $9.13 \text{ (mmol}_c \text{ L}^{-1})^{0.5}$). Most measured EC_e and SAR values were relatively low, posing no risk for crop production or indicating any risk of soil degradation. However, two profiles located in Alqueva (Odivelas Fase II), one with wheat (1.36 – 3.59 dS m^{-1} ; 3.76 – $9.13 \text{ (mmol}_c \text{ L}^{-1})^{0.5}$) and another with sugar beet (0.96 – 3.99 dS m^{-1} ; 5.71 – $8.78 \text{ (mmol}_c \text{ L}^{-1})^{0.5}$), registered

much larger EC_e and SAR values than the other soil profiles. Although these higher EC_e values could still be viable for growing crops moderately tolerant to soil salinity ($< 6.0 \text{ dS m}^{-1}$; Ayers and Westcot, 1985), these relatively high measured SAR values revealed serious management problems that should be addressed.

Luvisols (63 soil profiles) were well represented in the study area, being located in Caia, Lucefecit, Vigia, Odivelas, Roxo, and Alqueva (Odivelas Fase II, Monte Novo, Alvito-Pisão, Brinches, and Brinches-Enxoé). At the time, olive represented 12.3% of the characterized area, with maize, wheat, pasture, sugar beet, and melon (*Cucumis melo* L.) being also present. The measured EC_e values of the topsoil layers averaged 0.73 dS m^{-1} (Table 3), ranging from 0.10 to 5.08 dS m^{-1} . For the bottom layers and at different depths (> 25 cm), averages reached 0.67 – 1.25 dS m^{-1} , ranging from 0.09 to 5.93 dS m^{-1} . EC_e values were thus relatively low in most soil profiles, with some notable exceptions. Two soil profiles located in Roxo showed remarkably higher salinity values than all other profiles, with EC_e values reaching 2.15 – 5.93 dS m^{-1} at different depths. Also, six soil profiles in Alqueva (Odivelas Fase II) showed evidence of salt accumulation, with some having EC_e values of 1.41 – 2.05 dS m^{-1} at shallower depths (< 25 cm) while others registering values of 2.54 – 5.07 dS m^{-1} at deeper depths (> 50 cm). Hence, the measured EC_e values in the Luvisols reference group revealed large variability, reaching in some locations values that could affect the crop production of less tolerant crops to soil salinity. In these locations, the observed salinity build-up seemed again to be mostly associated with irrigation and fertilization management practices carried out throughout previous years, which may also have led to the degradation of soil characteristics as reflected by measured SAR values. For the topsoil layers, the measured SAR values averaged $2.09 \text{ (mmol}_c \text{ L}^{-1})^{0.5}$, ranging from 0.36 to $6.14 \text{ (mmol}_c \text{ L}^{-1})^{0.5}$. For the bottom layers, the measured SAR values averaged $2.69 \text{ (mmol}_c \text{ L}^{-1})^{0.5}$ at depths of 20–60 cm (ranging from 0.5 to $7.97 \text{ (mmol}_c \text{ L}^{-1})^{0.5}$), and $5.53 \text{ (mmol}_c \text{ L}^{-1})^{0.5}$ at depths below 60 cm (ranging from 0.42 to $16.09 \text{ (mmol}_c \text{ L}^{-1})^{0.5}$). The highest values were again found in Alqueva (Odivelas Fase II) and Roxo, but also in Odivelas and Alqueva (Monte Novo). In these locations, the measured SAR values showed an increasing trend with soil depth, increasing from 2.35 to $6.14 \text{ (mmol}_c \text{ L}^{-1})^{0.5}$ in the topsoil layers to 9.55 – $16.09 \text{ (mmol}_c \text{ L}^{-1})^{0.5}$ in the deeper layers.

Regosols (11 soil profiles) were found in Alqueva (Odivelas Fase II), Roxo, and Lucefecit. At the time, maize and pasture were the main land uses. The measured EC_e values were always lower than 1.3 dS m^{-1} (Table 3), constituting no risk for the crop production. Also, the SAR values were relatively low ($< 1.91 \text{ (mmol}_c \text{ L}^{-1})^{0.5}$), showing no risk of soil sodification.

Vertisols (27 soil profiles) were studied in Caia, Vigia, Lucefecit, and Alqueva (Odivelas Fase II, Brinches-Enxoé, Serpa, and Beringel-Serpa). Olive was the main land use in 14.8% of the sampled locations, with maize, wheat, sugar beet, and fallow representing the remaining areas. The measured EC_e values were again found to be relatively small, averaging between 0.52 – 0.58 dS m^{-1} at different depths (Table 3). Only one profile showed a notably higher value (2.15 dS m^{-1}) at lower depths. The measured SAR values were also relatively low, with averages varying between 0.54 – $1.63 \text{ (mmol}_c \text{ L}^{-1})^{0.5}$ at different depths (Table 3). However, two profiles located in Alqueva (Odivelas Fase II) showed SAR values higher than $5.0 \text{ (mmol}_c \text{ L}^{-1})^{0.5}$ at depths below 100 cm.

3.2. Soil salinization risks from current irrigation practices

Fig. 3 shows the simulated average EC_{sw} values at depths of 10, 50, 90, and 130 cm, as well as the range between the corresponding minimum and maximum values. Results are related to the S1 scenario, which considers irrigation practices currently carried out in very high-density olive orchards grown in the region. Also, results were grouped by soil reference groups (IUSS Working Group WRB, 2014) to reduce the large variability observed in model simulations, assuming thus that

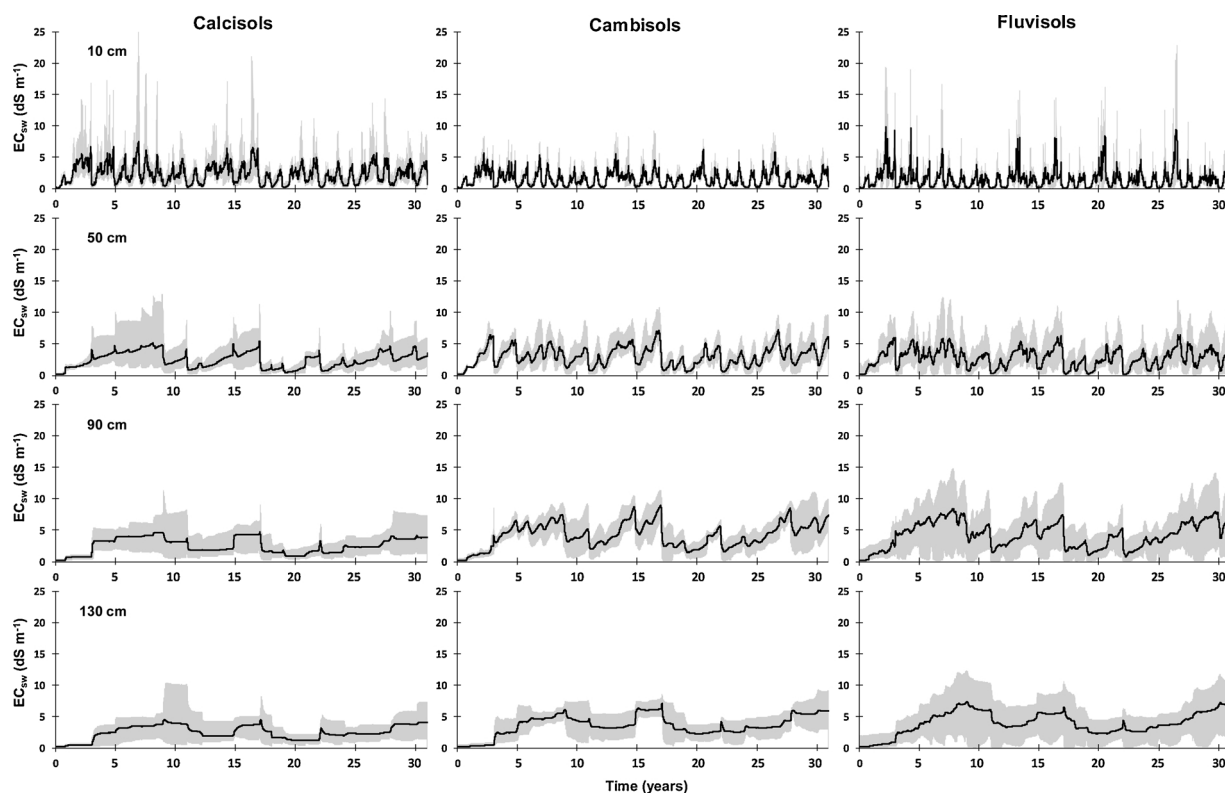


Fig. 3. (a) Average simulated values of the electrical conductivity of the soil solution (EC_{sw}) at 10, 50, 90, and 130 cm depth in Calcisols (15 profiles), Cambisols (4 profiles), and Fluvisols (40 profiles) (shaded areas represent range between maximum and minimum values). (b) Average simulated values of the electrical conductivity of the soil solution (EC_{sw}) at 10, 50, 90, and 130 cm depth in Luvisols (63 profiles), Regosols (11 profiles), and Vertisols (27 profiles) (shaded areas represent range between maximum and minimum values).

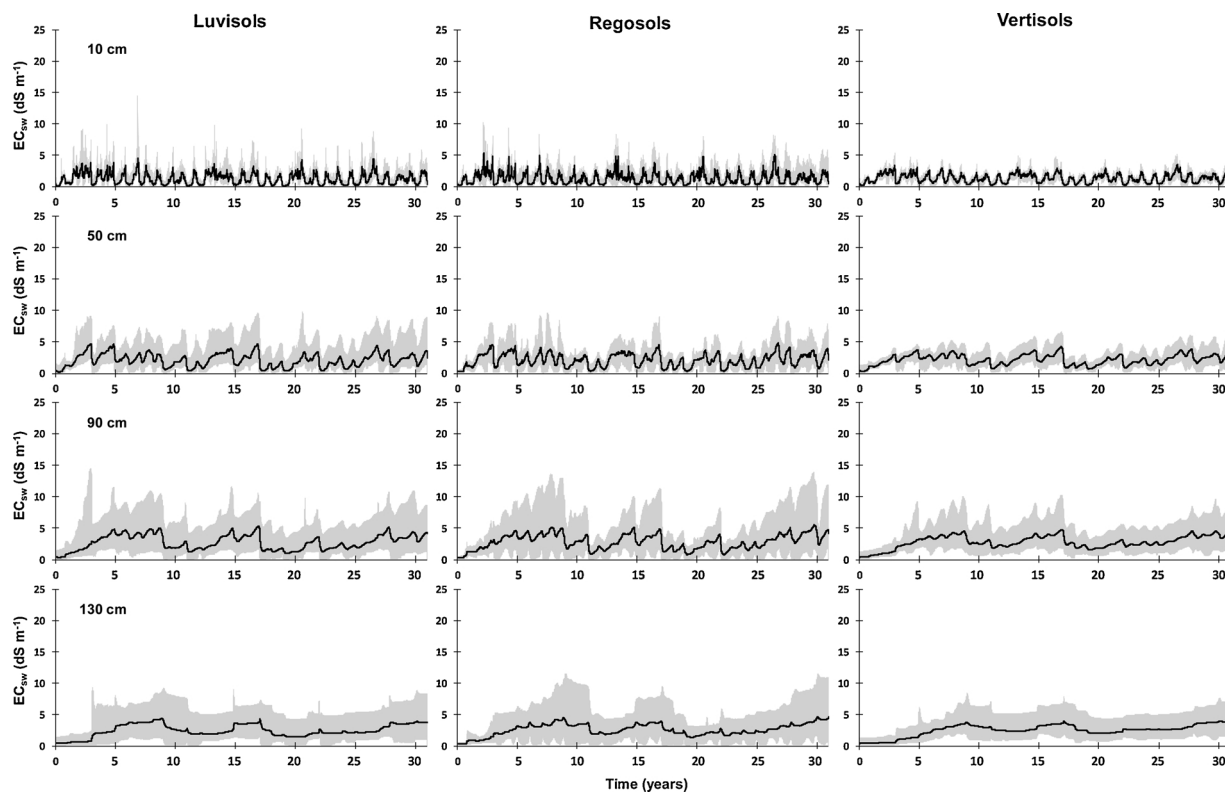


Fig. 3. (continued)

soil profiles in these classification groups possess, to some extent, similar physical and chemical characteristics, particularly in terms of soil horizons/layers, particle size distributions, soil structure, soil water retention, soil infiltration, and solute composition.

The EC_{sw} values showed a similar behavior in all topsoil layers (10 cm), increasing during the dry season due to irrigation (May to October) and then decreasing during the rainfall season (November to April) due to leaching, similarly as in Gonçalves et al. (2006) and Ramos et al. (2011, 2012). In some Calcisols and Fluvisols profiles, the EC_{sw} values regularly reached values higher than 12 dS m^{-1} ($EC_e = 6 \text{ dS m}^{-1}$) at the end of each irrigation season (Fig. 3a), thus exceeding the threshold limit for crops moderately tolerant to soil salinity (Ayers and Westcot, 1985), including the one set here for olive ($h_{\phi T} = -2975 \text{ cm}$; $EC_{sw} = 8 \text{ dS m}^{-1}$; $EC_e = 4 \text{ dS m}^{-1}$).

All soil reference groups showed evidence of salt accumulation at deeper depths ($\geq 50 \text{ cm}$), particularly during the years when annual rainfall amounts were smaller than the average. This happened in years 2–8 (1980–1986), 12–17 (1990–1995), 20–21 (1998–1998), and 26–27 (2004–2005) (Fig. 2), reflecting the large interannual variability of rainfall observed in Portugal and the frequent occurrence of drought spells in the region (Trigo and DaCamara, 2000; Paulo et al., 2012). In Calcisols (Fig. 3a), salt accumulation was more pronounced at a depth of 50 cm, reaching in some profiles values higher than 10 dS m^{-1} . At deeper depths, the higher permeability of the calcareous layers favored salt leaching. In Fluvisols (Fig. 3a), Luvisols (Fig. 3b), and Regosols (Fig. 3b), salt accumulation was more evident at depths below 50 cm, with some soil profiles, i.e., those with worse drainage conditions, showing EC_{sw} values above the threshold limit at depths of 90 cm. Cambisols (Fig. 3a) showed similar average results as soils in previous soil reference groups, with the analysis regarding variability being limited by the number of soil profiles available. In Vertisols (Fig. 3b), salt accumulation also occurred at depths below 50 cm during drier

years, but to a lesser extent.

The SAR values were more constant throughout the years (Fig. 4), not showing the same seasonal and interannual variability observed for EC_{sw} nor the same dependence on rainfall, similarly as in Gonçalves et al. (2006) and Ramos et al. (2011). After the 30-year simulation period, most soil reference groups continued exhibiting similar average SAR values as those determined from the initial soluble Na^+ , Ca^{2+} , and Mg^{2+} concentrations. The exceptions were Calcisols and Cambisols reference groups, which showed an increasing trend at different depths, although simulated averages always remained below $3.2 \text{ (mmol}_c \text{ L}^{-1})^{0.5}$. On the other hand, for the worst-case Fluvisols (Fig. 4a) and Luvisols (Fig. 4b), i.e., the soil profiles presenting initial higher SAR values, results showed the SAR values decreasing at different depths during the first 15 years of the simulation period. Explanations for this were surely related to the improved water quality considered in S1 (Table 1) compared to the one used in these locations. However, arguments related to the limitations in the model structure by not considering fertilization practices or some important biogeochemical process that would explain those higher SAR values might also be valid.

To summarize, the S1 results showed that despite the large variability observed in model simulations, particularly in Fluvisols, Luvisols, and Regosols, the average EC_{sw} values in all soil depths always remained below the threshold limit. No salt precipitation was ever observed, with the reported pIAP values (the negative logarithm of the ion activity product) indicating that conditions remained undersaturated with respect to calcite and gypsum (Truesdell and Jones, 1974). Also, apart from Calcisols and Cambisols, all other soil reference groups presented the average SAR values always within the same magnitude as the initial soil conditions. Based on these results, soil salinization and sodification risks resulting from current irrigation practices carried out in very high-density olive orchards can be considered low. Nonetheless, the variability of results necessitates the recommendation to closely

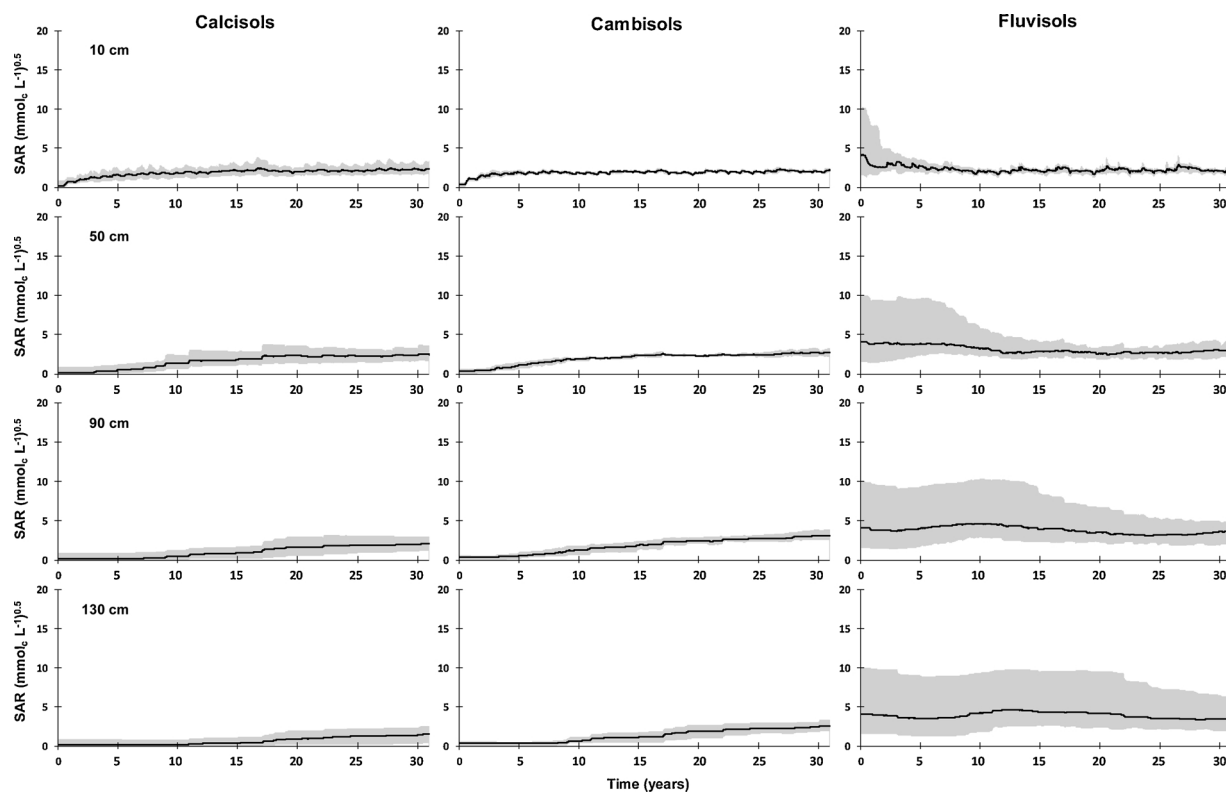


Fig. 4. (a) Average simulated values of the sodium adsorption ratio (SAR) at 10, 50, 90, and 130 cm depth in Calcisols (15 profiles), Cambisols (4 profiles), and Fluvisols (40 profiles) (shaded areas represent range between maximum and minimum values). (b) Average simulated values of the sodium adsorption ratio (SAR) at 10, 50, 90, and 130 cm depth in Luvisols (63 profiles), Regosols (11 profiles), and Vertisols (27 profiles) (shaded areas represent range between maximum and minimum values).

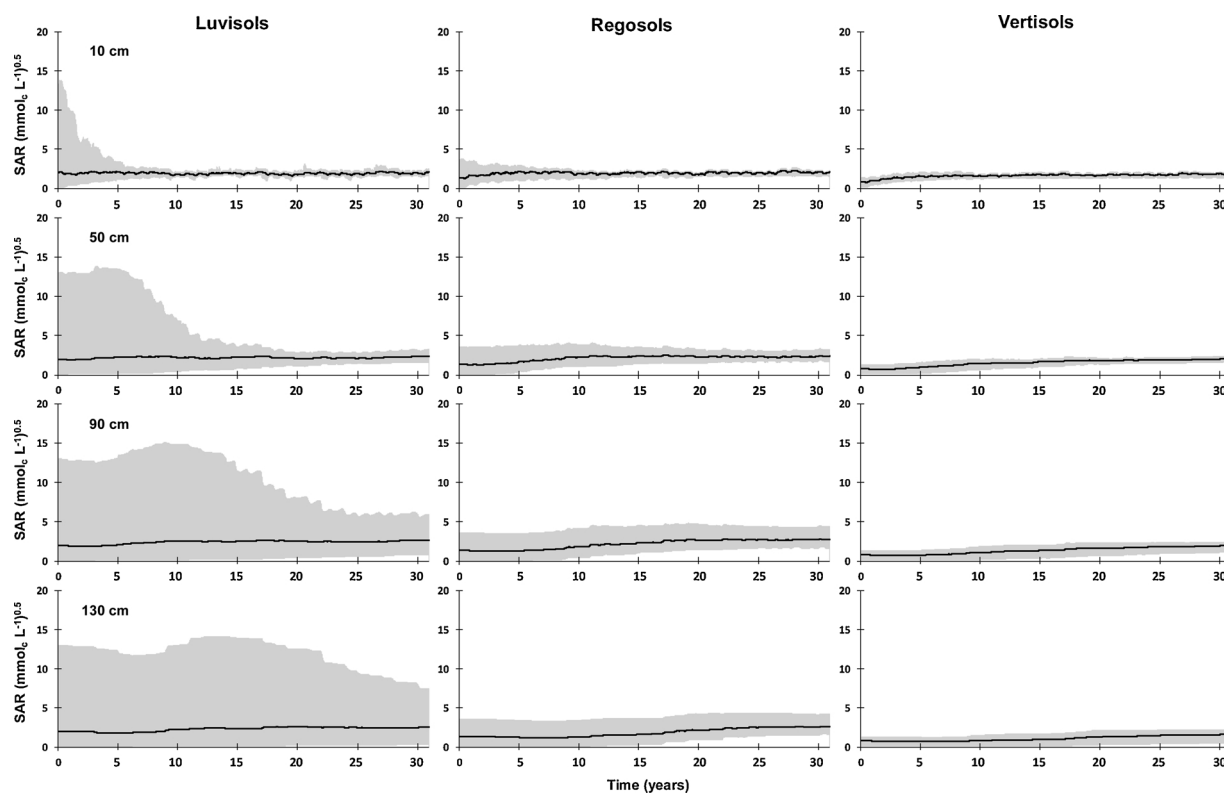


Fig. 4. (continued)

monitor the soil profiles most susceptible to soil salinization to prevent further degradation of soil resources in the region.

3.3. Scenario analysis

3.3.1. Soil salinization risks

Fig. 5 displays the box-plots of simulated EC_{sw} values for the S1-S8 scenarios at depths of 10, 50, 90, and 130 cm at the beginning of the simulation period (initial conditions) and at years 5, 10, 20, and 30. The results refer only to the salinity build-up at the end of a particular year's leaching season, just before the beginning of the next irrigation cycle. The analysis thus focuses only on comparing the final salinity levels for different scenarios over the years, without considering the EC_{sw} values during irrigation seasons, which may reach higher values than those discussed here.

Scenarios S2 and S3 with lower irrigation water quality produced slightly worse results than S1 (Table 1), with increasing EC_{sw} values due to the salinity build-up in the soil profile during dry years (years 2–8, 12–17, 20–21, and 26–27) and decreasing EC_{sw} values as a result of increased soil leaching during rainy years. As a result, although EC_{sw} were always higher than in S1, there was no gradual increase of EC_{sw} over the years. Even so, in most soil reference groups the EC_{sw} values remained below the threshold limit for crops moderately tolerant to soil salinity ($\text{EC}_{\text{sw}} < 12 \text{ dS m}^{-1}$), except during years 5 and 30 in all soil groups. In Fluvisols (Fig. 5b), the threshold limit was additionally also breached by the third quartile of simulation data at a depth of 90 cm during year 5 and a depth of 130 cm during years 10 and 30.

Scenarios S4 and S5 with even lower water quality, not commonly observed in the region except in smaller water reservoirs or during periods of water scarcity, showed the third quartile of the simulated EC_{sw} values regularly breaching the threshold limit for crops moderately tolerant to soil salinity at different depths in most soil reference groups. In Cambisols (Fig. 5a), this limit was breached even by the median of simulations at a depth of 90 cm during year 5. The worst predictions were obtained for Fluvisols (Fig. 5a), where the median of

simulated EC_{sw} values was frequently higher than the threshold limit at depths ≥ 90 cm.

Scenario S6 with the worse irrigation water quality, hardly observed in the region, produced the highest EC_{sw} values. Fluvisols (Fig. 5a) again registered the worst predictions, with the average EC_{sw} values often increasing above 15 dS m^{-1} at different depths.

The crop scenario S7, which considered maize as an alternative crop to olive, differed considerably from previous predictions, with the EC_{sw} values always remaining below those in S1 throughout the simulation period. The results thus confirmed the contribution of deficit irrigation practices to salt accumulation in the soil profile. For maize, where full irrigation practices are usually adopted (Cameira et al., 2003; Paredes et al., 2014; González et al., 2015; Ramos et al., 2017), soil salinity levels remained within the same magnitude as those determined at the beginning of the simulation period (i.e., the initial conditions) due to the higher irrigation amounts applied per year and per event, thus promoting to some extent salt leaching.

The climate change scenario S8, despite being relatively moderate by considering only a $0.8 \text{ }^\circ\text{C}$ increase in the average surface air temperature and a 30 mm decrease in the annual rainfall values, resulted in slightly higher EC_{sw} predictions than in S1. In most soil profiles, the simulated EC_{sw} values also remained always below the threshold limit for crops moderately tolerant to soil salinity. Nonetheless, the EC_{sw} values were significantly higher than in S1 following the rainy years 10 and 30. Reductions in annual rainfall amounts had thus an obvious negative effect on salt leaching, leading to greater soil salinization risks in the long term. Note that projected reductions in annual rainfall values were only considered between April and October, with rainfall increasing during winter months, in line with the Portuguese Local Warming Website Project (<https://portaldoclima.pt/en/>). However, this increase did not translate in larger percolation to promote soil leaching but, in most cases, in higher runoff.

Additionally, scenario S8 considered the same irrigation inputs as in S1. Although olive irrigation water requirements would be expected to increase only modestly due to higher ET_c rates (Tanasićević et al., 2014;

Valverde et al., 2015), additional irrigation amounts would inevitably lead to an increased salinity build-up as the leaching fraction would not be met to wash away accumulated salts from the root zone. S8 results further showed that larger rainfall reductions, as those considered in more extreme projections, would likely lead to an enhancement in the salinity build-up to levels that would undoubtedly affect olive development, particularly during extended drier periods. However, that would also be dependent on the rain distribution during the rainy season.

3.3.2. Soil sodification risks

Scenarios S1 and S2 produced comparable SAR results in all soil reference groups (Fig. 6), with S2 values generally increasing throughout the simulation period. For Calcisols (Fig. 6a) and Vertisols (Fig. 6b), the average SAR values reached a maximum of 3.10 and 2.53 ($\text{mmol}_c \text{L}^{-1} \text{0.5}$), respectively, at a depth of 50 cm. For Cambisols (Fig. 6a), Luvisols (Fig. 6b), and Regosols (Fig. 6b), the average SAR values reached a maximum of 3.72, 3.13, and 3.13 ($\text{mmol}_c \text{L}^{-1} \text{0.5}$), respectively, at a depth of 90 cm. The S2 results further showed the same SAR reduction trend for the worse-case profiles. However, the remaining profiles revealed increasing soil sodification levels in all soil depths. Only Fluvisols (Fig. 6a) showed a decrease in the average SAR values in the topsoil layers (≥ 50 cm), with the bottom layers maintaining similar results as those determined at the beginning of the simulation period (the initial condition).

The water quality scenarios S3 and S4 also produced comparable results, with all soil reference groups showing an increasing SAR trend until the end of the simulation period. In Calcisols ($6.00 \text{ (mmol}_c \text{L}^{-1} \text{0.5)}$), Cambisols ($6.87 \text{ (mmol}_c \text{L}^{-1} \text{0.5)}$), Fluvisols (7.70 (mmol_c

$\text{L}^{-1} \text{0.5)}$), Regosols ($5.87 \text{ (mmol}_c \text{L}^{-1} \text{0.5)}$), Luvisols ($6.00 \text{ (mmol}_c \text{L}^{-1} \text{0.5)}$), and Vertisols ($5.09 \text{ (mmol}_c \text{L}^{-1} \text{0.5)}$), the average maximum SAR values were again registered at depths of 50–90 cm. The same was observed for the water quality scenarios S5 and S6 but with the maximum average SAR values ranging from 10 to 15 ($\text{mmol}_c \text{L}^{-1} \text{0.5}$). Scenario S5 thus produced similar soil sodification levels as S6 due to the greater unbalance between Na^+ and $\text{Ca}^{2+} + \text{Mg}^{2+}$ in their irrigation waters (Table 1). The main difference was mostly in the time required to reach these maxima, with simulated averages being highest in S6 after 10 and 20 years, indicating that the sodification process occurred at a faster pace in S6 than in S5. Note that the SAR values at the end of simulations for scenarios S3–S6 were within the same order of magnitude as those found in some of the worse-case profiles in the region, indicating the need to improve future irrigation practices in the region to prevent further degradation of soil resources. Also, despite the higher SAR values in S5 and S6, salt precipitation never became a relevant process during the analysis.

In contrast to EC_{sw} , the crop scenario S7 produced an increase in the SAR values throughout the years in all soil reference groups. Nevertheless, the average SAR values remained always lower than 2.31 ($\text{mmol}_c \text{L}^{-1} \text{0.5}$, i.e., slightly below S1 predictions. Increased soil leaching due to different maize irrigation practices also ended up contributing to the removal of Na^+ from the root zone (Qadir et al., 2003), decreasing soil sodification risks. On the other hand, the climate change scenario S8 produced slightly higher SAR values in all soil reference groups than those reported for S1, remaining still below 3.91 ($\text{mmol}_c \text{L}^{-1} \text{0.5}$). Consequently, the S8 results suggested that climate change may contribute to the further degradation of soil resources in the region if management practices are not adjusted.

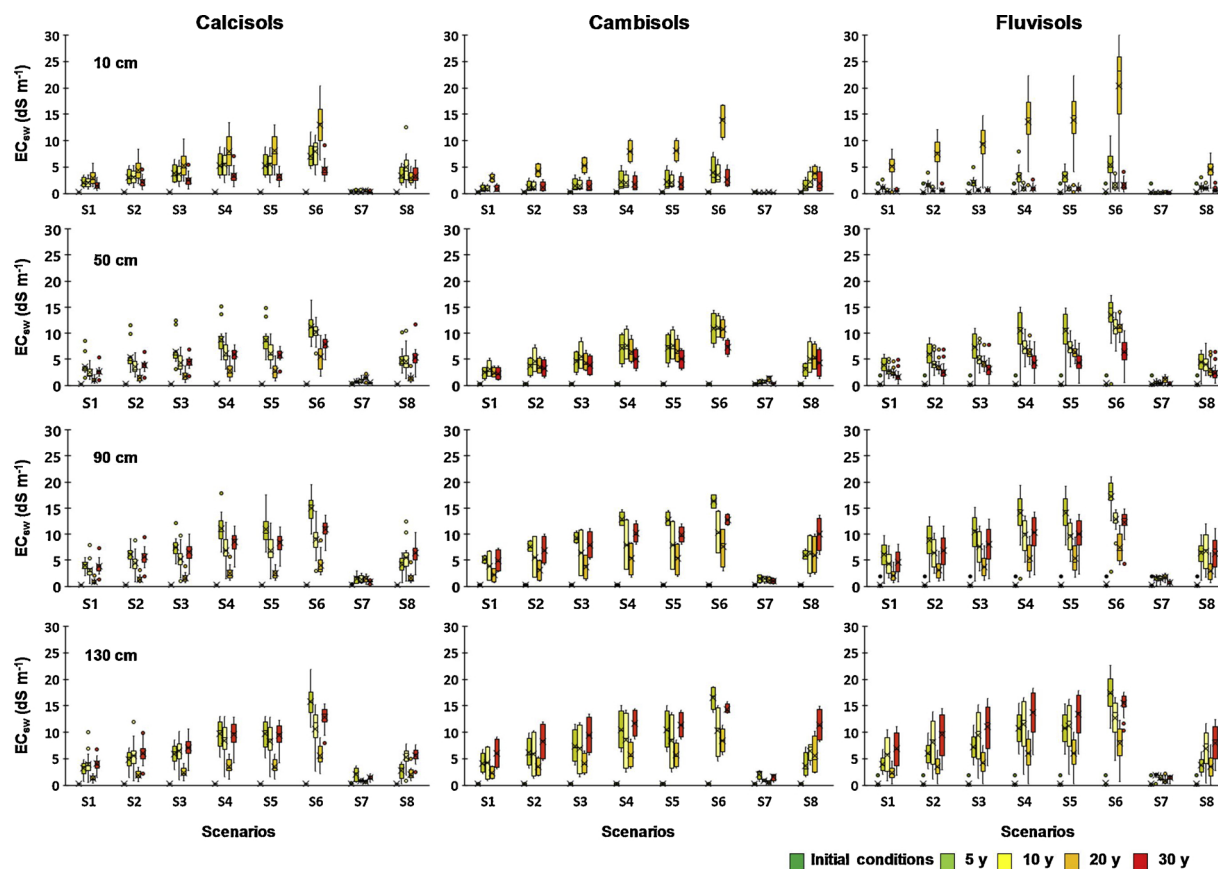


Fig. 5. (a) Box-plot of the evolution of the electrical conductivity of the soil solution (EC_{sw}) at 10, 50, 90, and 130 cm depth in Calcisols (15 profiles), Cambisols (4 profiles), and Fluvisols (40 profiles) and in different scenarios (S) after 5, 10, 20, 30 years (y). (b) Box-plot of the evolution of the electrical conductivity of the soil solution (EC_{sw}) at 10, 50, 90, and 130 cm depth in Luvisols (63 profiles), Regosols (11 profiles), and Vertisols (27 profiles) and in different scenarios (S) after 5, 10, 20, 30 years (y).

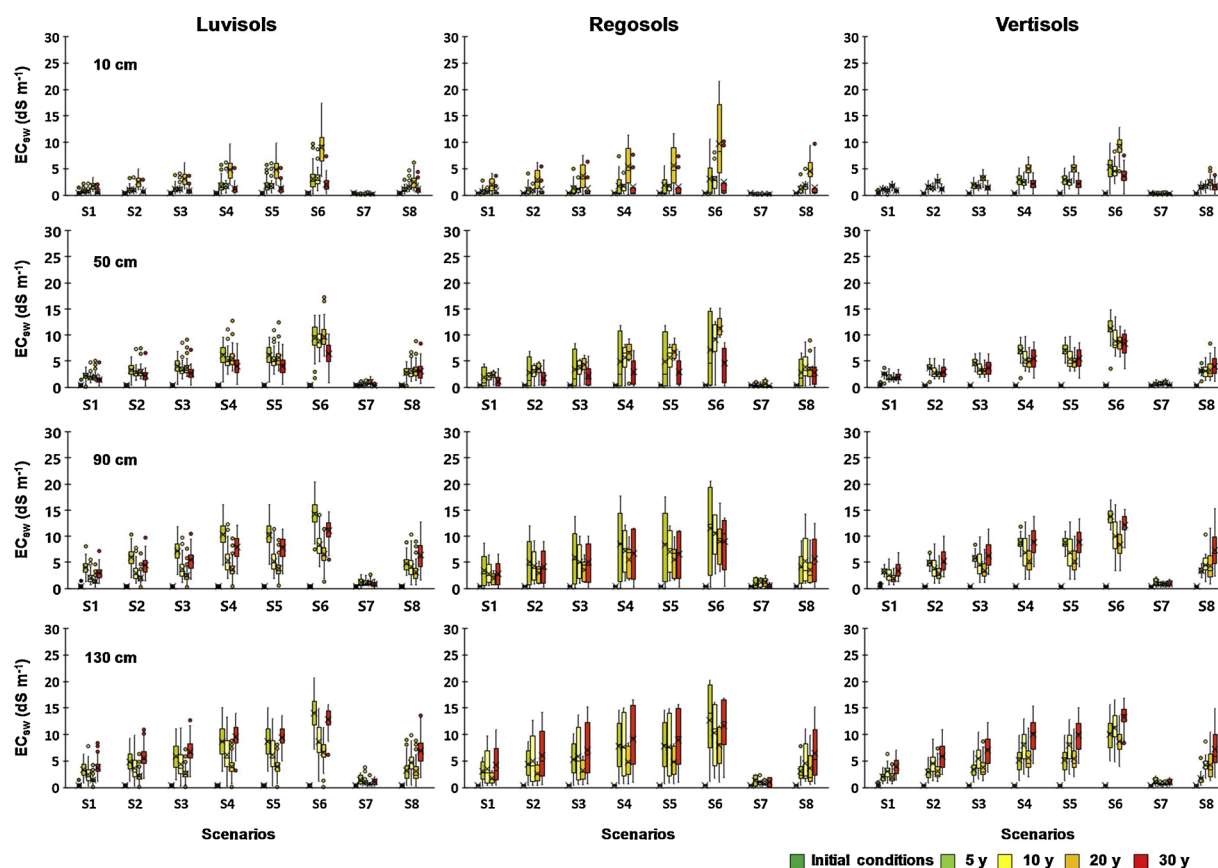


Fig. 5. (continued)

3.4. About model predictions

The EC_{sw} and SAR predictions presented above were associated with a large uncertainty as the modeling approach was not calibrated/validated in situ for each soil profile. Models generally require extensive calibration to assess if surface boundary conditions (i.e., potential evapotranspiration rates) are properly defined, water flow and solute transport are accurately described, and the problem at hand is suitably addressed by the model structure (Forkutsa et al., 2009; Rasouli et al., 2013; Xu et al., 2013; Cameira et al., 2014; González et al., 2015; Raji et al., 2016; Ramos et al., 2017). This is often accomplished by evaluating deviations between field observations and model predictions and, if necessary, adjusting model parameters to minimize these deviations. Validation then follows, again by comparing model predictions with an independent observation field dataset. Hence, model calibration/validation is a time-consuming and laborious process that could not be replicated for all studied locations.

Instead, the modeling approach adopted in this study followed closely Gonçalves et al. (2006) and Ramos et al. (2011, 2012), who extensively applied the HYDRUS software package (Šimůnek et al., 2016) for simulating multicomponent solute transport in a maize field located in the Alentejo region. In these studies, all input variables (i.e., the soil hydraulic properties, solute transport parameters, atmospheric demand, Gapon constants, physical and chemical characteristics of the soil, LAI, and root depth) were measured independently, resulting in model predictions reaching the root mean square errors (RMSE) of 0.03–0.04 $cm^3 cm^{-3}$ for soil water contents, 0.85–2.35 $dS m^{-1}$ for EC_{sw} , and 3.91–6.27 $(mmol_c L^{-1})^{0.5}$ for SAR. While these studies were conducted in maize fields, the HYDRUS software package has also been successfully tested for simulating soil water dynamics in high and very high-density olive orchards (Egea et al., 2016; Autovino et al., 2018), providing further background for this study (the RMSE values ranging

from 0.035–0.090 $cm^3 cm^{-3}$).

This study further relied on inputs from available data sources on measured soil hydraulic properties for the soil profiles included in this study (Gonçalves et al., 2011; Ramos et al., 2017). These parameters were determined in the laboratory on soil samples of a certain size, being likely less representative of actual flow conditions, transport, and reaction processes occurring at the field scale due to limitations in the porous media continuum. As a result, simulation errors, as those given earlier, are usually relatively larger than when soil hydraulic parameters are calibrated in situ by minimizing deviations between model simulations and field observations (González et al., 2015; Ramos et al., 2017; Karandish and Šimůnek, 2018). This is even more relevant for soils with a high clay content, where the role of macropores on soil water dynamics can only be accurately described using dual-porosity/dual-permeability models (e.g., Šimůnek and van Genuchten, 2008).

Additionally, soil hydraulic data were also complemented with information estimated from regional PTFs using the particle size distribution as inputs (Ramos et al., 2014b), which are known to produce RMSEs ranging from 0.038–0.058 $cm^3 cm^{-3}$ for water retention at different matric heads and 0.588 for $\log(K_s)$. However, these PTFs have never been evaluated for simulating water flow under field conditions, bringing additional uncertainty to model predictions. Likewise, solute transport simulations were indirectly estimated using soil PTFs from Gonçalves et al. (2002) that were developed based on a very limited number of samples (24).

Limitations related to model structure errors should also be addressed while analyzing model results. First, the more accurate axisymmetric or three-dimensional representations of flow and solute transport under drip irrigation (Lazarovitch et al., 2005; Hanson et al., 2008; Kandelous et al., 2011; Ramos et al., 2012; Egea et al., 2016; Autovino et al., 2018) were not adopted in this study. In drip irrigation, irrigation volumes and salts are not uniformly applied over the soil

surface as considered in the one-dimensional modeling approach carried out here. Salts tend to accumulate below the dripper, from where they are then transported downwards and sideways depending on irrigation volumes and frequency, rainfall, evapotranspiration rates, and soil hydraulic properties. Thus, such simplification can lead to inaccurate results in the short term, with the salinity build-up and the salinity stress in the root zone being most likely overestimated (Hanson et al., 2008). However, the relevance of this simplification was assumed to be reduced in this long-term study (30 years), mostly because results were considered only at the end of the leaching season when salts could be assumed to be more evenly distributed in the soil profile, and their accumulation extends farther than just below the drip emitter, approximating then a 1D solution as in Ramos et al. (2012). Nonetheless, future studies should overcome this limitation, namely by developing field datasets capable of validating modelling applications that use more complex representations of the soil domain. Even if salts redistribute horizontally with time their distribution along the soil horizon in a real three-dimensional soil system will never be as uniform as the one considered in a 1D solution. To demonstrate this point, we used HYDRUS (2D/3D) (Šimůnek et al., 2016) to simulate the development of the salinity profile in an axisymmetrical three-dimensional soil profile with a radius of 67.5 and a depth of 150 cm for the same irrigation and climate conditions (S1 scenario) as used in one-dimensional simulations (Fig. 7). Fig. 7 shows that while (due to winter rainfalls) soil salinities are in the long term relatively uniform in the top soil layer, salts tend to accumulate more under trees than inter-row in deeper soil layers.

Second, this study considered similarly as Gonçalves et al. (2006); Ramos et al. (2011), and Raji et al. (2016) the feasibility of the multicomponent transport modeling approach embedded in the HYDRUS

software package (Šimůnek et al., 2016) for quantifying soil salinization and sodification risks from irrigation practices. Cation exchange reactions were considered to be well described by the Gapon exchange equations. Also, precipitation/dissolution reactions were assumed to be reasonably well accounted for using the available multicomponent kinetic expressions.

The effects of the salinity build-up on the unsaturated soil hydraulic properties were also not considered in this study. This factor has so far been considered only in a limited number of studies (e.g., Gonçalves et al., 2006; Mallants et al., 2017). The HYDRUS software package accounts for the adverse effects of salt accumulation on the soil hydraulic conductivity by using reduction functions developed by McNeal (1968) that depend on the salinity and SAR levels. Mallants et al. (2017) applied this approach to hypothetical scenarios in which non-conventional irrigation waters with high concentrations of total dissolved solids and high SAR values were used, but results were never validated using field data. Gonçalves et al. (2006) also applied this approach in their lysimeters studies but the simulation period was too short and concentrations too low to provide an insight on the effect of soil salinity on soil hydraulic properties. Consequently, the approach used in HYDRUS for considering the effect of salt accumulation on soil hydraulic properties remains to be validated, and for that purpose, it was not adopted here. Nevertheless, the relevance of this process for the objectives of this study is not disputed. Salt accumulation (particularly, Na⁺ and K⁺) often leads to clay dispersion, swelling, flocculation, and overall degradation of soil physicochemical properties, reducing, as a result, the soil hydraulic conductivity, infiltration rate, and soil water retention. As such, EC_{sw} and SAR predictions would likely be aggravated if the effects of salt accumulation on soil hydraulic properties were considered. Likewise, fertilization practices were not included in

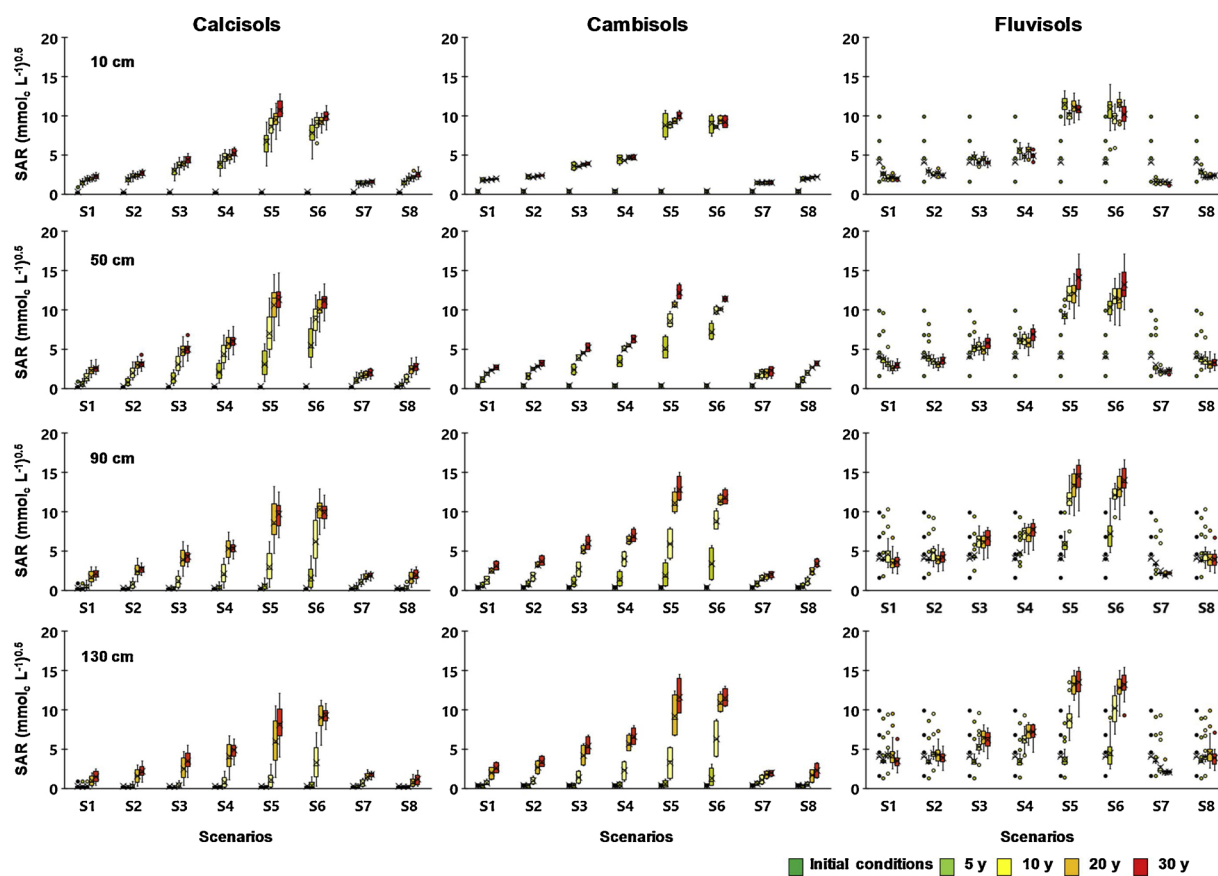


Fig. 6. (a) Box-plot of the evolution of the sodium adsorption ratio (SAR) at 10, 50, 90, and 130 cm depth in Calcisols (15 profiles), Cambisols (4 profiles), and Fluvisols (40 profiles) and in different scenarios (S) after 5, 10, 20, 30 years (y). (b) Box-plot of the evolution of the sodium adsorption ratio (SAR) at 10, 50, 90, and 130 cm depth in Luvisols (63 profiles), Regosols (11 profiles), and Vertisols (27 profiles) and in different scenarios (S) after 5, 10, 20, 30 years (y).

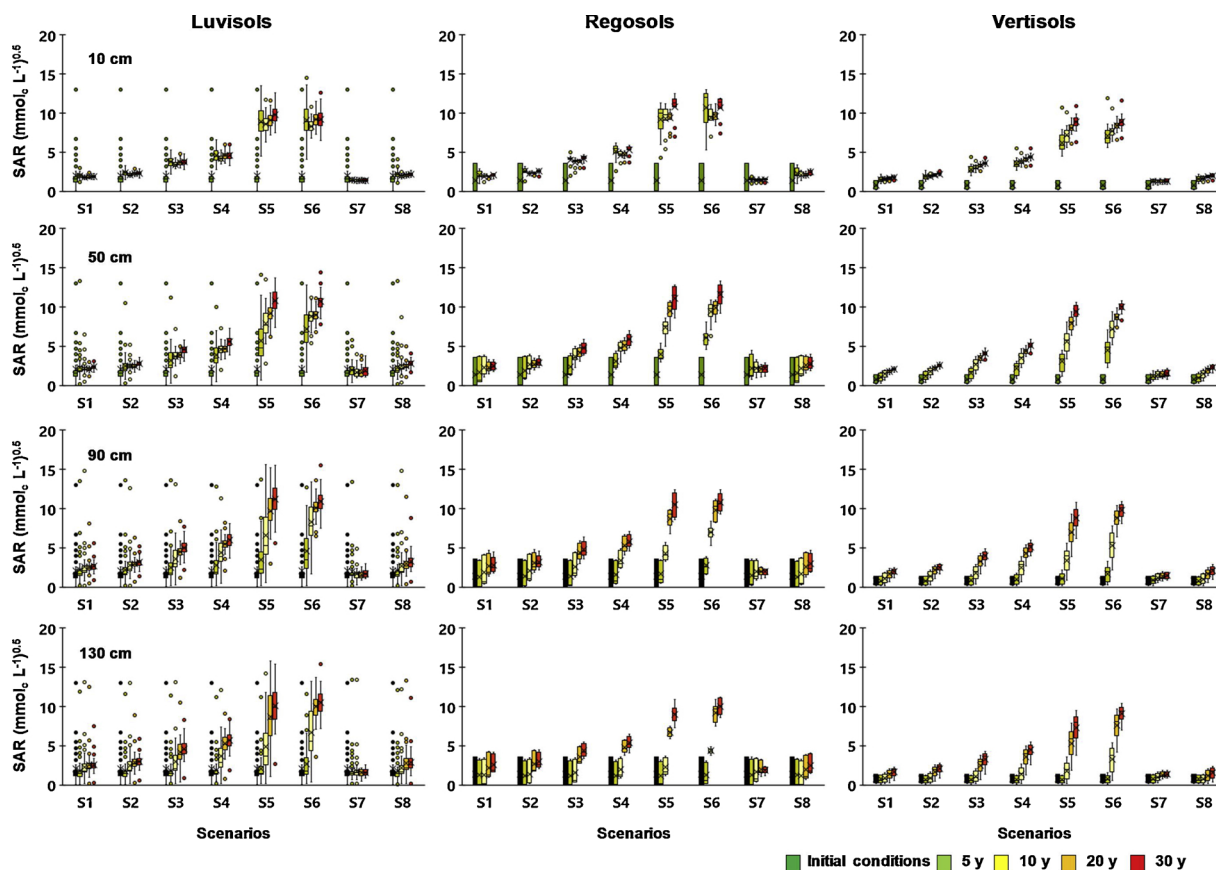


Fig. 6. (continued)

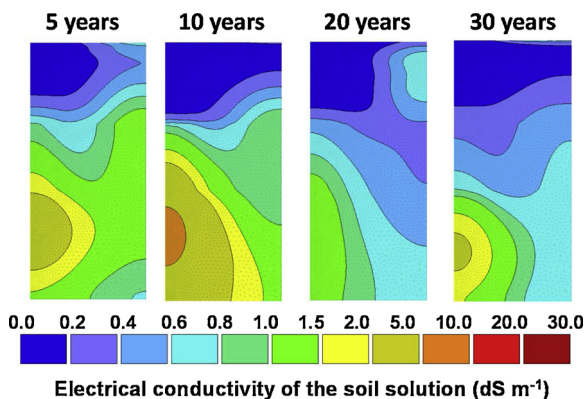


Fig. 7. Spatial distribution of the electrical conductivity of the soil solution in a Fluvisol (axisymmetric representation of the soil profile with a radius of 67.5 cm and a depth of 150 cm; the wetted radius ≈ 10 cm located in the top left corner of each salinity profile; the root distribution with the maximum rooting radius and depth of 67 and 120 cm, respectively).

model simulations, which, if considered, would likely also increase EC_{sw} values in all scenarios.

Despite all limitations, the adopted modeling approach provided a certain degree of confidence in EC_{sw} and SAR predictions, being based on modeling concepts that have been the focus of extensive research over the last few decades (Šimůnek et al., 2014, 2016), with most being successfully tested in the Alentejo region (Gonçalves et al., 2006; Ramos et al., 2011, 2012). Anyhow, these limitations discussed above only emphasize the need for regular monitoring of soil salinization/sodification risks in the Alentejo region since even the most advance modeling approach will always be a mere simplification of the processes and details involved, and of nature’s variability. There is thus the need to

include new data sources, management practices, and tools to assess further the impact of deficit irrigation practices carried out in very high-density olive orchards (≥ 1000 trees ha^{-1}) grown in the Alentejo region on local soil resources. There is also the need for extending this research to high-density olive orchards (≥ 200 trees ha^{-1}), where the impact of the intensive management practices on soil resources also deserves a more detailed analysis. With the intensification of agriculture, it is thus further critical to extend this study to other Mediterranean crops such as vine grapes, fruit trees, horticultural and protein crops, for which irrigation introduced substantial changes in their production systems or made possible their implementation in the region. This research should focus not only on soil salinization/sodification, but also on other soil degradation processes which likewise threaten the sustainability of agricultural production in the region (Masselink et al., 2017; Cerdà et al., 2018; Di Prima et al., 2018; Rodrigo-Comino et al., 2018a, 2018b). Only then the sustainability of the Mediterranean agriculture systems can be achieved, and the United Nations Sustainable Development Goals can be met (Keesstra et al., 2016; UN, 2018).

4. Conclusions

The Alentejo region in southern Portugal has recently experienced a major land use change, with the area with high and very-high density olive orchards expanding rapidly over the last few years. This has also led to great changes in the management of soil and water resources, with deficit irrigation practices being now often adopted to maximize yields and the quality of olive oils. As a result, soil salinization and sodification problems can potentially increase in a region where rainfall may not be sufficient to leach the accumulated salts during irrigation.

Before the expansion of olive orchards, different soil survey studies revealed relatively low soil salinization and sodification levels in the

region, with several exceptions being found, particularly in Fluvisols and Luvisols, as a result of erroneous management practices.

The scenario based on current irrigation practices in very high-density olive orchards (S1) showed reduced risks of soil salinization, with simulated average EC_{sw} values at the end of the leaching seasons (i.e., at the end of the irrigation cycles) always remaining below the salinity threshold limit for olive and for most crops moderately tolerant to soil salinity. Likewise, soil sodification risks were considered to be generally quite low, with the simulated average SAR values being also kept within the same magnitude of those determined at the beginning of the simulation period.

The scenarios based on the expected deterioration of the quality of irrigation waters (S2-S6) produced higher salinization/sodification levels, with some closely matching the worse EC_{sw} and SAR values found for baseline conditions (i.e., before the establishment of olive orchards). Olive deficit irrigation practices (S1) also resulted in worse indicators than those obtained when considering maize as an alternative crop (S7). The full irrigation practice, commonly used for maize, with larger water depths per event and season, helped in reducing the salinity build-up in the soil profile. Climate change (S8) also contributed to the increase in soil salinization/sodification levels, with EC_{sw} and SAR values being always slightly higher than those simulated for current conditions (S1). Climate change projections considered in this study were very modest, involving only a 0.8 °C increase in the average value of the surface air temperature and a 30 mm decrease in the corresponding annual rainfall amounts. For more extreme projections, the dependency of EC_{sw} on annual rainfall showed that soil salinization levels would likely increase if larger rainfall reductions were considered. On the other hand, SAR predictions would not be much affected.

Finally, the results displayed a relatively large variability in all soil reference groups and scenarios. Model predictions were also associated with large uncertainties as the HYDRUS-1D model was not calibrated/validated in situ for each soil profile, relying on existing datasets, auxiliary tools (PTFs), and on past research carried out in the region. Nonetheless, model predictions presented here should not be taken lightly as the risk of soil salinization/sodification is real. There is thus the need to closely monitor the problem at the local scale to prevent further degradation of soil and water resources in the region.

Acknowledgments

This research was performed within the Project SOIL4EVER (Increasing water productivity through the sustainable use of soils, PTDC/ASP-SOL/28796/2017) of the Fundação para a Ciência e Tecnologia (FCT). MARETEC acknowledges the national funds from FCT (Project UID/EEA/50009/2019). T. B. Ramos was supported by the FCT grant SFRH/BPD/110655/2015.

References

- Ahmed, C.B., Magdich, S., Ben Rouina, B., Boukhris, M., Ben Abdullah, F., 2012. Saline water irrigation effects on soil salinity distribution and some physiological responses of field grown Chemlali olive. *J. Environ. Manag.* 113, 538–544.
- Ahumada-Orellana, L.E., Ortega-Farías, S., Searles, P.S., 2018. Olive oil quality response to irrigation cut-off strategies in super high-density orchard. *Agric. Water Manag.* 202, 81–88.
- Allen, R.G., Pereira, L.S., 2009. Estimating crop coefficients from fraction of groundcover and height. *Irrig. Sci.* 28, 17–34.
- Allen, R.G., Pereira, L.S., Raes, D., Smith, M., 1998. *Crop Evapotranspiration – Guidelines for Computing Crop Water Requirements*. Irrig. Drain. FAO, Rome, Italy, pp. 56.
- Aragüés, R., Guillén, M., Royo, A., 2010. Five-year growth and yield response of two young olive cultivars (*Olea europea* L., cvs. Arbequina and Empeltre) to soil salinity. *Plant Soil* 334, 423–432.
- Autovino, D., Rallo, G., Provenzano, G., 2018. Predicting soil and plant water status dynamics in olive orchards under different irrigation systems with HYDRUS-2D: model performance and scenario analysis. *Agric. Water Manag.* 203, 225–235.
- Ayers, R., Westcot, D., 1985. *Water Quality for Agriculture*. Irrig. Drain. FAO, Rome, pp. 29.
- Cameira, M.R., Fernando, R.M., Pereira, L.S., 2003. Monitoring water and NO₃-N in irrigated maize fields in the Sorraia Watershed, Portugal. *Agric. Water Manag.* 60 (3), 199–216.
- Cameira, M.R., Pereira, A., Ahuja, L., Ma, L., 2014. Sustainability and environmental assessment of fertigation in an intensive olive grove under Mediterranean conditions. *Agric. Water Manag.* 146, 346–360.
- Cerdà, A., Rodrigo-Comino, J., Giménez-Morera, A., Keesstra, S.D., 2018. Hydrological and erosional impact and farmer's perception on catch crops and weeds in citrus organic farming in Canyoles river watershed, Eastern Spain. *Agric. Ecosyst. Environ.* 258, 49–58.
- Conceição, N., Tezza, L., Häusler, M., Lourenço, S., Pacheco, C.A., Ferreira, M.I., 2017. Three years of monitoring evapotranspiration components and crop and stress coefficients in a deficit irrigated intensive olive orchard. *Agric. Water Manag.* 191, 138–152.
- DGADR, 2018. *Aproveitamento hidroagrícolas do Grupo II no Continente. Culturas Regadas em 2017*. Direção Geral de Agricultura e do Desenvolvimento Rural, Ministério da Agricultura, Florestas e Desenvolvimento Rural, Lisboa.
- Di Prima, S., Rodrigo-Comino, J., Novara, A., Iovino, M., Pirastru, M., Keesstra, S., Cerdà, A., 2018. Soil physical quality of citrus orchards under tillage, herbicide, and organic managements. *Pedosphere* 28 (3), 463–477.
- Dominguez, A., Tarjuelo, J.M., de Juan, J.A., López-Mata, E., Breidy, J., Karam, F., 2011. Deficit irrigation under water stress and salinity conditions: the MOPECO-Salt Model. *Agric. Water Manag.* 98, 1451–1461.
- EDIA, 2018. *Empresa de Desenvolvimento e Infraestruturas do Alqueva*. Beja, Portugal <http://www.edia.pt/en/> (Last accessed 24.07.2018).
- Egea, G., Diaz-Espejo, A., Fernández, J.E., 2016. Soil moisture dynamics in a hedgerow olive orchard under well-watered and deficit irrigation regimes: assessment, prediction and scenario analysis. *Agric. Water Manag.* 164, 197–211.
- FAOSTAT, 2018. *Food and Agriculture Organization of the United Nations*. Rome, Italy <http://www.fao.org/faostat/en/#home> (Last accessed 24.07.18).
- Feddes, R.A., Kowalik, P.J., Zaradny, H., 1978. *Simulation of Field Water Use and Crop Yield*. Simulation Monographs Pudoc., Wageningen, The Netherlands.
- Forokutsa, I., Sommer, R., Shirokova, Y.I., Lamers, J.P.A., Kienzler, K., Tischbein, B., Martius, C., Vlek, P.L.G., 2009. Modeling irrigated cotton with shallow groundwater in the Aral Sea Basin of Uzbekistan: II. Soil salinity dynamics. *Irrig. Sci.* 27, 319–330.
- Ghrab, M., Gargouri, K., Bentaher, H., Chartzoulakis, K., Ayadi, M., Ben Mimoun, M., Masmoudi, M.M., Mechli, N.B., Psarras, G., 2013. Water relations and yield of olive tree (cv. Chemali) in response to partial root-zone drying (PRD) irrigation technique and salinity under arid climate. *Agric. Water Manag.* 123, 1–11.
- Gómez-del-Campo, M., 2013. Summer deficit-irrigation strategies in a hedgerow olive orchard cv. 'Arbequina': effect on fruit characteristics and yield. *Irrig. Sci.* 31, 259–269.
- Gonçalves, M.C., Leij, F.J., Schaap, M.G., 2002. Pedotransfer functions for solute transport parameters of Portuguese soils. *Eur. J. Soil Sci.* 52, 563–574.
- Gonçalves, M.C., Šimůnek, J., Ramos, T.B., Martins, J.C., Neves, M.J., Pires, F.P., 2006. Multicomponent solute transport in soil lysimeters with waters of different quality. *Water Resour. Res.* 42, W08401. <https://doi.org/10.1029/2005WR004802>.
- Gonçalves, M.C., Ramos, T.B., Pires, F.P., 2011. Base de dados georreferenciada das propriedades do solo. In: Coelho, P.S., Reis, P. (Eds.), *Agrorural. Contributos Científicos*. Instituto Nacional dos Recursos Biológicos, Oeiras, Portugal, pp. 564–574.
- González, M.G., Ramos, T.B., Carlesso, R., Paredes, P., Petry, M.T., Martins, J.D., Aires, N.P., Pereira, L.S., 2015. Modelling soil water dynamics of full and deficit drip irrigated maize cultivated under a rain shelter. *Biosyst. Eng.* 132, 1–18.
- GPAa, 2004. *Alqueva Agrícola – Plano de Intervenção*. Direção Geral de Agricultura e do Desenvolvimento Rural, Ministério da Agricultura, Florestas e Desenvolvimento Rural, Lisboa, Portugal (Last accessed 24.07.18). <http://sir.dgadr.gov.pt/plano-int-alqueva>.
- Gucci, R., Fereres, E., Goldhamer, D.A., 2012. Olive. In: Steduto, P., Hsiao, T.C., Fereres, E., Raes, D. (Eds.), *Crop Yield Response to Water*. Irrig. Drain. Food and Agriculture Organization of the United Nations, Rome, pp. 300–315 Paper 66.
- Hanson, B.R., Šimůnek, J., Hopmans, J.W., 2008. Leaching with subsurface drip irrigation under saline, shallow ground water conditions. *Vadose Zone J.* 7, 810–818.
- Hernández, M.L., Velásquez-Palmer, D., Sicardo, M.D., Fernández, J.E., Diaz-Espejo, A., Martínez-Rivas, J.M., 2018. Effect of a regulated deficit irrigation strategy in a hedgerow 'Arbequina' olive orchard on the mesocarp fatty acid composition and desaturase gene expression with respect to olive oil quality. *Agric. Water Manag.* 204, 100–106.
- IUSS Working Group WRB, 2014. *World Reference Base for Soil Resources 2014. International Soil Classification System for Naming Soils and Creating Legends for Soil Maps*. World Soil Resources Reports No. 106. FAO, Rome.
- Jacques, D., Šimůnek, J., Mallants, D., van Genuchten, M.Th., 2018. The HPX software for multicomponent reactive transport during variably-saturated flow: Recent developments and applications. *J. Hydrol. Hydromech.* 66 (2), 211–226.
- Kandelous, M.M., Šimůnek, J., van Genuchten, M.Th., Malek, K., 2011. Soil water content distributions between two emitters of a subsurface drip irrigation system. *Soil Sci. Soc. Am. J.* 75, 488–497.
- Karandish, F., Šimůnek, J., 2018. An application of the water footprint assessment to optimize production of crops irrigated with saline water: a scenario assessment with HYDRUS. *Agric. Water Manag.* 208, 67–82.
- Keesstra, S.D., Bouma, J., Wallinga, J., Titttonell, P., Smith, P., Cerdà, A., Montanarella, L., Quinton, J.N., Pachepsky, Y., van der Putten, W.H., Bardgett, R.D., Moolenaar, S., Mol, G., Jansen, B., Fresco, L.O., 2016. The significance of soils and soil science towards realization of the United Nations Sustainable Development Goals. *Soil* 2, 111–128.
- Lazarovitch, N., Šimůnek, J., Shani, U., 2005. System-dependent boundary condition for water flow from subsurface source. *Soil Sci. Soc. Am. J.* 69, 46–50.
- Lorite, J.J., Gabaldón-Leal, C., Ruiz-Ramos, M., Belaj, A., de la Rosa, R., León, L., Santos, C., 2018. Evaluation of olive response and adaptation strategies to climate change under semi-arid conditions. *Agric. Water Manag.* 204, 247–261.
- Maas, E.V., 1990. Crop salt tolerance. In: In: Tanji, K.K. (Ed.), *Agricultural Salinity Assessment and Management*. Manual Eng. Pract., vol. 71. Am. Soc. of Civ. Eng.,

- Reston, VA, pp. 262–304.
- Maas, E.V., Hoffman, G.J., 1977. Crop salt tolerance-current assessment. *J. Irrig. Drain. Div. Am. Soc. Civ. Eng.* 103, 115–134.
- Mallants, D., Šimůnek, J., Torkzaban, S., 2017. Determining water quality requirements of coal seam gas produced for sustainable irrigation. *Agric. Water Manage.* 189, 52–69.
- Masselink, R.J.H., Temme, A.J.A.M., Giménez, R., Casali, J., Keesstra, S.D., 2017. Assessing hillslope-channel connectivity in an agricultural catchment using rare-earth oxide tracers and random forests models. *Cuad. Investig. Geográfica* 43, 19–39.
- McNeal, B.L., 1968. Prediction of the effect of mixed-salt solutions on soil hydraulic conductivity. *Soil Sci. Soc. Am. Proc.* 32, 190–193.
- McNeal, B.L., Oster, J.D., Hatcher, J.T., 1970. Calculation of electrical conductivity from solution composition data as an aid to in-situ estimation of soil salinity. *Soil Sci.* 110, 405–414.
- Melgar, J.C., Mohamed, Y., Serrano, N., García-Galavís, P.A., Navarro, C., Parra, M.A., Benlloch, M., Fernández-Escobar, R., 2009. Long term responses of olive trees to salinity. *Agric. Water Manage.* 96, 1105–1113.
- Mualem, Y., 1976. A new model for predicting the hydraulic conductivity of unsaturated porous media. *Water Resour. Res.* 12, 513–522.
- Murillo, J.M., López, R., Fernández, J.E., Cabrera, F., 2000. Olive tree response to irrigation with wastewater from the table olive industry. *Irrig. Sci.* 19, 175–180.
- Oster, J.D., Letey, J., Vaughan, P., Wu, L., Qadir, M., 2012. Comparison of transient state models that include salinity and matric stress effects on plant yield. *Agric. Water Manage.* 103, 167–175.
- Paço, T.A., Pôças, I., Cunha, M., Silvestre, J.C., Santos, F.L., Paredes, P., Pereira, L.S., 2014. Evapotranspiration and crop coefficients for a super intensive olive orchard. An application of SIMDualKc and METRIC models using ground and satellite observations. *J. Hydrol.* 519, 2067–2080.
- Pang, X.P., Letey, J., 1998. Development and evaluation of ENVIRO-GRO, an integrated water, salinity, and nitrogen model. *Soil Sci. Soc. Am.* 62, 1418–1427.
- Paredes, P., Melo-Abreu, J.P., Alves, I., Pereira, L.S., 2014. Assessing the performance of the AquaCrop model to estimate maize yields and water use under full and deficit irrigation with focus on model parameterization. *Agric. Water Manage.* 144, 81–97.
- Paulo, A.A., Rosa, R.D., Pereira, L.S., 2012. Climate trends and behaviour of drought indices based on precipitation and evapotranspiration in Portugal. *Nat. Hazards Earth Syst. Sci.* 12, 1481–1491.
- Peragón, J.M., Pérez-Latorre, J., Delgado, A., Tóth, T., 2018. Best management irrigation practices assessed by a GIS-based decision tool for reducing salinization risks in olive orchards. *Agric. Water Manage.* 202, 33–41.
- Pereira, L.S., Gonçalves, J.M., Dong, B., Mao, Z., Fang, S.X., 2007. Assessing basin irrigation and scheduling strategies for saving irrigation water and controlling salinity in the upper Yellow River Basin, China. *Agric. Water Manage.* 93, 109–122.
- Qadir, M., Steffens, D., Yan, F., Schubert, S., 2003. Sodium removal from a calcareous saline-sodic soil through leaching and plant uptake during phytoremediation. *Land Degrad. Develop.* 14, 301–307.
- Ragab, R., Malash, N., Abdel Gawad, G., Arslan, A., Ghaibeh, A., 2005. A holistic generic integrated approach for irrigation, crop and field management: 1. The SALTMED model and its application using field data from Egypt and Syria. *Agric. Water Manage.* 78 (1–2), 67–88.
- Raij, I., Šimůnek, J., Ben-Gal, A., Lazarovitch, N., 2016. Water flow and multicomponent solute transport in drip irrigated lysimeters: experiments and modeling. *Water Resour. Res.* 52, 6557–6574. <https://doi.org/10.1002/2016WR018930>.
- Ramos, A.F., Santos, F.L., 2009. Water use, transpiration, and crop coefficients for olives (cv. Cordovil) grown in orchards in Southern Portugal. *Biosyst. Eng.* 102, 321–333.
- Ramos, A.F., Santos, F.L., 2010. Yield and olive oil characteristics of a low-density orchard (cv. Cordovil) subjected to different irrigation regimes. *Agric. Water Manage.* 97 (2), 363–373.
- Ramos, T.B., Šimůnek, J., Gonçalves, M.C., Martins, J.C., Prazeres, A., Castanheira, N.L., Pereira, L.S., 2011. Field evaluation of a multicomponent solute transport model in soils irrigated with saline waters. *J. Hydrol.* 407, 129–144.
- Ramos, T.B., Šimůnek, J., Gonçalves, M.C., Martins, J.C., Prazeres, A., Pereira, L.S., 2012. Two-dimensional modeling of water and nitrogen fate from sweet sorghum irrigated with fresh and blended saline waters. *Agric. Water Manage.* 111, 87–104.
- Ramos, T.B., Gonçalves, M.C., Brito, D., Martins, J.C., Pereira, L.S., 2013. Development of class pedotransfer functions for integrating water retention properties into Portuguese soil maps. *Soil Res.* 51, 262–277.
- Ramos, T.B., Horta, A., Gonçalves, M.C., Martins, J.C., Pereira, L.S., 2014a. Development of ternary diagrams for estimating water retention properties using geostatistical approaches. *Geoderma* 230, 229–242.
- Ramos, T.B., Gonçalves, M.C., Martins, J.C., Pereira, L.S., 2014b. Comparação de diferentes funções de pedotransferência para estimar as propriedades hidráulicas dos solos em Portugal. In: Gonçalves, M.C., Ramos, T.B., Martins, J.C. (Eds.), *Livro de Actas do Encontro Anual da Sociedade Portuguesa da Ciência do Solo*, 26 to 28 June. Instituto Nacional de Investigação Agrária e Veterinária, Oeiras, pp. 29–34.
- Ramos, T.B., Horta, A., Gonçalves, M.C., Pires, F.P., Duffy, D., Martins, J.C., 2017. The INFOSOLO database as a first step towards the development of a soil information system in Portugal. *Catena* 158, 390–412.
- Ramos, T.B., Simionesei, L., Jauch, E., Almeida, C., Neves, R., 2017a. Modelling soil water and maize growth dynamics influenced by shallow groundwater conditions in the Sorraia Valley region, Portugal. *Agric. Water Manage.* 185, 27–42.
- Rasouli, F., Pouya, A.K., Šimůnek, J., 2013. Modeling the effects of saline water use in wheat-cultivated lands using the UNSATCHEM model. *Irrig. Sci.* 31, 1009–1024.
- Ritchie, J.T., 1972. Model for predicting evaporation from a row crop within complete cover. *Water Resour. Res.* 8, 1204–1213.
- Roberts, T., Lazarovitch, N., Warrick, A.W., Thompson, T.L., 2009. Modeling salt accumulation with subsurface drip irrigation using HYDRUS-2D. *Soil Sci. Soc. Am. J.* 73, 233–240.
- Rodrigo-Comino, J., Davis, J., Keesstra, S.D., Cerdà, A., 2018a. Updated measurements in vineyards improves accuracy of soil erosion rates. *Agron. J.* 110, 1–7.
- Rodrigo-Comino, J., Taguas, E., Seeger, M., Ries, J.B., 2018b. Quantification of soil and water losses in an extensive olive orchard catchment in southern Spain. *J. Hydrol.* 556, 749–758.
- Rosa, R.D., Ramos, T.B., Pereira, L.S., 2016. The dual Kc approach to assess maize and sweet sorghum transpiration and soil evaporation under saline conditions: application of the SIMDualKc model. *Agric. Water Manage.* 115, 291–310.
- Rosecrance, R.C., Krueger, W.H., Milliron, L., Bloese, J., Garcia, C., Mori, B., 2015. Moderate regulated deficit irrigation can increase olive oil yields and decrease tree growth in super high density ‘Arbequina’ olive orchards. *Sci. Hortic.* 190, 75–82.
- Santos, F.L., Valverde, P.C., Ramos, A.F., Reis, J.L., Castanheira, N.L., 2007. Water use and response of a dry-farmed olive orchard recently converted to irrigation. *Biosyst. Eng.* 98 (1), 102–114.
- Šimůnek, J., Hopmans, J.W., 2009. Modeling compensated root water and nutrient uptake. *Ecol. Modell.* 220, 505–521.
- Šimůnek, J., Suarez, D.L., 1994. Two-dimensional transport model for variably saturated porous media with major ion chemistry. *Water Resour. Res.* 30, 1115–1133.
- Šimůnek, J., van Genuchten, M.Th., 2008. Modeling nonequilibrium flow and transport processes using HYDRUS. *Vadose Zone J.* 7 (2), 782–797. <https://doi.org/10.2136/VZJ2007.0074>.
- Šimůnek, J., Šejna, M., Saito, H., Sakai, M., van Genuchten, M.Th., 2013. The HYDRUS-1D software package for simulating the one-dimensional movement of water, heat, and multiple solutes in variably-saturated media: Version 4.16. Dep. Environ. Sci. University of California, Riverside.
- Šimůnek, J., Jacques, D., Ramos, T.B., Leterme, B., 2014. The use of multicomponent solute transport models in environmental analyses. In: Teixeira, W.G., Ceddia, M.B., Ottoni, M.V., Donnagema, G.K. (Eds.), *Application of Soil Physics in Environmental Analyses: Measuring, Modelling and Data Integration*. Springer, pp. 377–402.
- Šimůnek, J., van Genuchten, M.Th., Šejna, M., 2016. Recent developments and applications of the HYDRUS computer software packages. *Vadose Zone J.* 15 (7). <https://doi.org/10.2136/vzj2016.04.0033>.
- Skaggs, T.H., van Genuchten, M.Th., Shouse, P.J., Poss, J.A., 2006. Macroscopic approaches to root water uptake as a function of water and salinity stress. *Agric. Water Manage.* 86, 140–149.
- SNIRH, 2018. Serviço Nacional de Informação dos Recursos Hídricos. Agência Portuguesa do Ambiente, Lisboa, Portugal (Last accessed 12.12.2018). <https://snirh.apambiente.pt/>.
- Stocker, T.F., Qin, D., Plattner, G.-K., Alexander, L.V., Allen, S.K., Bindoff, N.L., Bréon, F.-M., Church, J.A., Cubasch, U., Emori, S., Forster, P., Friedlingstein, P., Gillett, N., Gregory, J.M., Hartmann, D.L., Jansen, E., Kirtman, B., Knutti, R., Krishna Kumar, K., Lemke, P., Marotzke, J., Masson-Delmotte, V., Meehl, G.A., Mokhov, I.I., Piao, S., Ramaswamy, V., Randall, V., Rhein, M., Rojas, V., Sabine, C., Shindell, D., Talley, L.D., Vaughan, D.G., Xie, S.-P., 2013. Technical summary. In: Stocker, T.F., Qin, D., Plattner, G.-K., Tignor, M., Allen, S.K., Boschung, J., Nauels, A., Xia, Y., Bex, V., Midgley, P.M. (Eds.), *Climate Change 2013: The Physical Science Basis*. Contribution of Working Group I to the Fifth Assessment Report of the Intergovernmental Panel on Climate Change. Cambridge University Press, Cambridge, United Kingdom and New York, NY, USA.
- Tanasijevic, L., Todorovic, M., Pereira, L.S., Pizzigalli, C., Lionello, P., 2014. Impacts of climate change on olive crop evapotranspiration and irrigation requirements in the Mediterranean region. *Agric. Water Manage.* 144, 54–68.
- Tekaya, M., Mechri, B., Dabbaghi, O., Mahjoub, Z., Laamari, S., Chihouai, B., Boujnah, D., Hammami, M., Chehab, H., 2016. Changes in key photosynthetic parameters of olive trees following soil tillage and wastewater irrigation modified olive oil quality. *Agric. Water Manage.* 178, 180–188.
- Tognetti, R., d’Andria, R., Morelli, G., Alvino, A., 2005. The effect of deficit irrigation on seasonal variations of plant water use in *Olea europaea* L. *Plant Soil* 273, 139–155.
- Trigo, R.M., daCamara, C.C., 2000. Circulation weather types and their influence on the precipitation regime in Portugal. *Int. J. Climatol.* 20, 1559–1581.
- Truesdell, A.H., Jones, B.F., 1974. Wateq, a computer program for calculating chemical equilibria of natural waters. *J. Res. U. S. Geol. Surv.* 2, 233–248.
- U.S. Salinity Laboratory Staff, 1954. *Diagnosis and Improvement of Saline and Alkali Soils*. USDA Handbook 60, Washington, USA.
- UN, 2018. *United Nations Sustainable Development Goals*. United Nations, NY (Last accessed 12.12.18). <https://www.un.org/sustainabledevelopment/>.
- Valverde, P., Serralheiro, R., Carvalho, M., Maia, R., Oliveira, B., Ramos, V., 2015. Climate change impacts on irrigated agriculture in the Guadiana river basin (Portugal). *Agric. Water Manage.* 152, 17–30.
- Van Dam, J.C., Groenendijk, P., Hendriks, R.F.A., Kroes, J.G., 2008. Advances of modeling water flow in variably saturated soils with SWAP. *Vadose Zone J.* 7, 640–653.
- van Genuchten, M.Th., 1980. A closed form equation for predicting the hydraulic conductivity of unsaturated soils. *Soil Sci. Soc. Am. J.* 44, 892–898.
- van Genuchten, M.Th., 1987. A Numerical Model for Water and Solute Movement in and Below the Root Zone. Res. Rep. 121. U.S. Salinity Laboratory, USDA, ARS, Riverside, California.
- Villalobos, F.J., Orgaz, F., Testi, K., Fereres, E., 2000. Measurement and modeling of evapotranspiration of olive (*Olea europaea*, L.) orchards. *Eur. J. Agron.* 13, 155–163.
- Wesseling, J.G., Elbers, J.A., Kabat, P., van den Broek, B.J., 1991. SWATRE: Instructions for Input. Report. Winand Staring Cent., Wageningen, Netherlands.
- White, N.L., Zelazny, L.M., 1986. Charge properties in soil colloids. In: Sparks, D.L. (Ed.), *Soil Physical Chemistry*. CRC Press, Boca Raton, Fla, pp. 39–81.
- Xu, X., Huang, G., Sun, C., Pereira, L.S., Ramos, T.B., Huang, Q., Hao, Y., 2013. Assessing the effects of water table depth on water use, soil salinity and wheat yield: searching for a target depth for irrigated areas in the upper Yellow River basin. *Agric. Water Manage.* 125, 46–60.